ANALYSIS OF THE URBAN THERMAL ENVIRONMENT ASSOCIATED WITH SOCIO ECONOMIC CONDITIONS IN JAKARTA, INDONESIA USING SATELLITE REMOTE SENSING

衛星リモートセンシングを用いたインドネシア・ジャカルタ市における熱環境と社会経済条件の比較分析

September 2014

Hasti Widyasamratri

ANALYSIS OF THE URBAN THERMAL ENVIRONMENT ASSOCIATED WITH SOCIO ECONOMIC CONDITIONS IN JAKARTA, INDONESIA USING SATELLITE REMOTE SENSING

YAMANASHI UNIVERSITY GRADUATE SCHOOL JOINT
MEDICAL ENGINEERING DEPARTMENT

DOCTORAL COURSE DISSERTATION

September 2014

Hasti Widyasamratri

ABSTRACT

ANALYSIS OF THE URBAN THERMAL ENVIRONMENT ASSOCIATED WITH SOCIO ECONOMIC CONDITIONS IN JAKARTA, INDONESIA USING SATELLITE REMOTE SENSING

Hasti Widyasamratri

Indonesia population has reached 225 million by 2006 (Indonesia statistic bureau, 2006) and more than 50 % population is concentrated in Java island which comprises about 7 % of the total land area. Rapid growth of population is triggering to high intensive urbanization and environmental problem in the big city such as Jakarta. The urbanization is characterized by change of agricultural to non-agricultural activities and can be associated by change of vegetation to impervious surfaces. Less vegetation area in urban areas, which would bring air temperature rise and high density of transportation, is found to be the most important cause of urban heat island in Jakarta. High concentration of population in urban areas can aggravate the urban environmental condition. In some developed areas, dense ground meteorological sites are installed to measure air temperature (T_a) in 1.5 – 2 m height above the ground. However, this condition is relatively difficult to apply in developing areas.

The usage of remote sensing satellite to detect physical component including thermal condition in a large spatial area has been widely known. Thermal infra-red remote sensing data is one of the satellite data sources that can help to determine surface temperature (T_S) from the space. It can provide large scale area on earth surface distribution data and the isolated area even it cannot calculate detail information of temperature. T_a components are governed from the earth-atmosphere balance, such as absorption of incoming solar radiation, emission of infrared long wave radiation and the sensible-latent heat loss. These T_a components are connected to T_S that can be extracted from thermal sensor in satellite remote sensing

Thermal environment status in urban area, which extracted remote sensing data, and its relation with urban socioeconomic condition become the objectives of this research.

Firstly, we investigated land cover at Jakarta in 1989 and 2006 to understand the distribution of land surface features in urban areas. The result shows that the built-up areas are growing to the outer city while vegetation areas are decreased. The thermal environment, observed by direct measurement (September – October 2012), shows the features of urban heat island at Jakarta, which were characterized by high air temperature in the city center at night time. Thermal environment in Jakarta has been

influenced by the sea breezes from the Java sea in the northern area, and the mountainous in the southern area.

Secondly, to estimate T_a from satellite-derived T_S, we applied simple regression (SR) method to Landsat data in 1989 and 2006. From the comparison between ground-based observation of T_S and T_a, it was shown that they are correlated strongly enough to use that data to T_a estimation ($R^2 = 0.74$). The minimum value of T_a estimated in 1989 was 20.11 °C, maximum value was 35.62 °C, and standard deviation was (SD) 5.93 °C. In 2006, the minimum was 31.8 °C, maximum value was 37.6 °C, and standard deviation was 6.35 °C. Large standard deviation in these results shows that this method still needs to be improved.

To improve the method, we tested simple regression and surface energy balance (SEB) method into MODIS (2012 dry season) data. In the estimated value by SR method with MODIS data, the RMSE at night time was 15.53 °C, the minimum value was 19.62°C, and maximum value was 22.49 °C, respectively. In daytime, RMSE was 11.69°C, and minimum value 21.55°C, and maximum value was 31.55°C (appeared in the city center). To reduce the error in T_a estimation, we also applied the SEB method to the same data sets. In the estimated value by SEB method using MODIS data, the RMSE value at the night time was 11.36°C, the minimum value was 23.43°C, and the maximum value was 25°C. In the daytime, the RMSE value was 9.75°C, the minimum value was 25°C, and the maximum value was 30°C. From these results, it was shown that the biases in SEB method were smaller than those in SR method.

Lastly, to detect the relationship between urban thermal environment and socio economic conditions in Jakarta, we combined physical and socioeconomic variables into urban livelihood indices. We used T_a as the physical variable; and we used population, family using electricity, health insurance certificate for poor family, and poor family certificate as the socioeconomic variables. Weighted analysis and overlay technique in ArcGIS was used in this step. Averaged T_a derived from MODIS data sets has close correlation with population except at 1 am. From this relationship, T_a and population are combined and represented by environment index. Low environment index is detected mainly in inner urban both at the nighttime and daytime (36.1% at nighttime and 29.6% in daytime). Socioeconomic index is created by overlaying socioeconomic variables from PODES 2010 except population data; and it represents household and population welfare in study area. In Jakarta, 45.9% areas, where 37.7% families are living, are dominated by fair socioeconomic index. Urban environment livelihood index is the synthesis result from environment index and socioeconomic index in study area. We found that the urban center in Jakarta has low environmental livelihood which was characterized by low environment and high socioeconomic quality.

This study revealed the effectiveness of remote sensing data to estimate T_a in a large scale as an order to overcome the spatial lack of ground meteorological measurement and use the result as the physical parameter to detect urbanization. The SEB method estimates T_a better than SR method and it showed good performance in MODIS data. We also show that the combined index of thermal status and socioeconomic parameters is effective to evaluate the urban livelihood.

要約

衛星リモートセンシングを用いたインドネシア・ジャカルタ市における
熱環境と社会経済条件の比較分析

ハスティ　ウィディヤサムラトリ

インドネシアの人口は 2006 年までに（インドネシア統計局、2006 年）225 百万人に達し、50％以上の人口が総面積の約 7％を占めるジャワ島に集中している。都市化は、農地のそれ以外の土地利用への改変によって特徴付けられ、それは植生域の不浸透面への変化につながる。気温上昇や交通の過密化をもたらす都市部での植生減少は、ジャカルタのヒートアイランドの最も重要な原因であることが指摘されている。都市部の過密な人口も都市環境条件を悪化させうる。一部の開発地域では、地上から高さ 2～1.5m の気温（Ta）を測定する地上気象観測点が密に設置されている。しかし、このような密な地上観測点の設置は、発展途上国では困難である。

また、大きな空間スケールでの熱環境を含む物理的な要素を検出するために衛星リモートセンシングが広く利用されている。地表面温度（T_S）の空間分布については衛星による熱赤外線リモートセンシングデータより推定可能である。Ta は、地表面に入射する太陽放射の吸収、長波放射の放出、顕熱潜熱による損失などの熱収支により決まっている。これらの Ta を決定する要素は、衛星リモートセンシングから抽出可能な TS から推定することが可能である。

以上を踏まえて、本研究では衛星リモートセンシングによる都市熱環境の抽出、および熱環境と社会経済的条件との比較分析を目的とする。

第一に、我々は、都市部における土地表面の特徴の分布を把握するために 1989 年と 2006 年にジャカルタで土地被覆を推定した。その結果、市街地が外側へ拡大し、植生領域が減少したことを示した。直接測定による熱環境観測（2012 年 9 月-10 月）から、特に夜間の市内中心部における高い気温によって特徴づけられた、ジャカルタにおけるヒートアイランドの特徴が捉えられた。ジャカルタでの熱環境は、北部地域ではジャワ海からの潮風の、南部地域では山岳地帯の影響を受けていることがわかった。

第二に、衛星リモートセンシングから抽出された T_S から Ta を推定するために、我々は 1989 年と 2006 年の Landsat 衛星データに単回帰（SR）法を適用した。地上観測より得られた T_S と Ta の比較から、それらは Ta の推定に使用するのに十分な強い相関を持っている（R^2= 0.74）ことが示された。1989 年における Ta 推定値の最小値は 20.11℃であり、最大値は 35.62℃であり、標準偏差（SD）は 5.93℃であった。2006 年

では、最小値は 31.8℃、最大値は 37.6℃、標準偏差は 6.35℃であった。これらの結果における大きな標準偏差より、この手法は、改善の余地があると考えられる。

手法を改善するために、我々は 2012 年乾季における MODIS データに単回帰と地表面エネルギー収支（SEB）法を適用した。SR 法を MODIS データに適用した推定値では、夜間の Ta について RMSE は 15.53℃、最大値は 22.49℃、最小値は 19.62℃であった。昼間の Ta については、RMSE は 11.69℃であり、最小値は 21.55℃であり、最大値は（市の中心部で見られた）31.55℃であった。続いて Ta の推定における誤差を低減するために、同じデータセットに SEB 法を適用した。SEB 法を MODIS データに適用した推定値では、夜間の Ta について RMSE 値は 11.36℃、最小値は 23.43℃、最大値は 25.00℃であった。昼間の Ta については、RMSE 値は 9.75° C、最小値は 25℃であり、最大値は 30℃であった。これらの結果から、SEB 方法におけるバイアスが SR 方式のものよりも小さいことが示された。

最後に、ジャカルタの都市熱環境と都市化との関係を検出するために、物理的および社会経済的変数を組み合わせた都市生活指標を検討する。物理的な変数として Ta を使用し、社会経済的変数として、人口、電気を利用できる世帯数、貧困家庭用健康保険を活用している世帯数、貧困家庭の認定を受けている世帯数を使用した。重み付け分析および ArcGIS のオーバーレイ技術を活用した。MODIS データセットから推定した平均気温（Ta）は午前 1 時を除いて、人口と密接な相関関係を示した。この関係より、Ta と人口を結合し、環境指標として表す。低い環境指標は、夜間（36.1％）と昼間（29.6％）の両方で都市域の内側で検出された。社会経済指標は、PODES2010 から人口データを除いた社会経済的変数を組み合わせることによって作成され、調査地域における世帯の豊さを表す。ジャカルタで世帯数の 37.7％が居住している 45.9％の領域において、良好な社会経済指標が見られた。都市生活指標は調査地域において環境指標と社会経済指標を合成して作成したものである。その検討を通じて、ジャカルタの中心部は、低い環境指標と高い社会経済指標により特徴づけられた低い都市生活指標を示すことが明らかとなった。

本研究では、地上気象測定の空間的不足を克服し、都市化を検出するために必要な物理的なパラメータである広域での Ta を推定するために、リモートセンシングデータの活用が有効であることを示した。SEB 方法は、SR 方式よりも Ta を良く推定することが可能であり、MODIS データへの適用において良好な性能を示した。また、熱的、社会経済的変数を組み合わせた指標が、都市生活を評価する有効な指標であることを示した。

ACKNOWLEDGEMENTS

I would like to express my deepest gratitude to the Lord for his guidance and strength. I would like to express my sincere gratitude to my supervisor Assoc. Prof. Kazuyoshi Souma for his guidance, support and encouragement throughout the course of graduate study at University of Yamanashi. I would like to thank also Prof. Tadashi Suetsugi, Assoc. Prof. Yutaka Ichikawa, Assoc. Prof. Hiroshi Ishidaira, and Assoc. Prof. Hiroshi Kobayashi for their meaningful guidance as members of supervising committee. I am grateful to Assistant Prof. Jun Magome for his suggestion during my research work here. I am also grateful to all GCOE members, staffs and colleagues for their suggestions, support and facilitation during my study here.

I owe my gratitude to many people who shared their expertise and friendship. These include Dr. Kazuhiro Kakizawa, Dr. Ichiko Inagaki, Dr. Masakazu Hashimoto, Nurul Nadia, Ayaka Watanabe, and all Suikou members. My Indonesian friends in Kofu who have been through all the happy and sad times, Dr. Ratih Indri Hapsari, Dr. Yureana Wijayanti, Dr. Risky Ayu Kristanti, Anang Faturochman, Purna Sophie, Febrina Hartanti, and Octavina Naa. I would like to thank also Prof. Suhartono, Dr. Suharyadi, Dr. Arief Kusumawanto as my supervisor in Gadjah Mada University, thank you for the online discussion. My classmate members in Gadjah Mada University, thank you for the sharing.

I am very grateful to the GCOE program of University of Yamanashi and Japanese government (MEXT scholarship) in providing me financial support during my graduate studies.

Finally, I would like to express my biggest and special gratitude to my brother and parents, Hariyadi Djamal., M. T, and Asih Priyanti who always support me in every single time. Mr. Sarjono and families, Mr. Yukihiko Sakatani and families, Mr. A. Ouchi and families, their supports are uncountable. Thank you for all my friends here that I can not mention one by one. Thank you for those who come and go in my life. You have written many stories which encourage me during my life in Japan. Thank you.

TABLE OF CONTENTS

LIST OF FIGURES

LIST OF TABLES

LIST OF ABBREVIATIONS

DHF : Dengue hemorrhagic fever.

DKI : Daerah khusus ibukota.

EI : Environment index.

JMA : Jakarta metropolitan area.

LST : Land surface temperature.

MODIS : Moderate resolution imaging spectrometer.

RMSE : Root mean square error.

SI : Socioeconomic index.

Ta : Air temperature.

TIR : Thermal infra red.

T_S : Surface temperature.

WHO : World Health Organization.

UHI : Urban heat island.

ULI : Urban livelihood index.

CHAPTER I

INTRODUCTION

1. 1. Urban Development in Jakarta city

Urbanization has various impacts on the urban environment. The population of Jakarta, the capital of Indonesia, was approximately 12 million in 2000 while it was only 5 million in the 1970s. In 2010, 43% of the Asia-Pacific population lived in urban areas of Jakarta (UN-ESCAPE, 2011). With the rapid population increase, the urban area also expanded rapidly within the past several decades, which may have strongly affected the local climate of the area. Jakarta's urban fringe is growing faster than the city itself. The present Jakarta and its extended surrounding zone (Jakarta special region, Bogor, Tangerang, Bekasi) cover total 7500 km^2, namely Jakarta Metropolitan Area (JMA) or Jabodetabek (Jakarta, Bogor, Tangerang, and Bekasi). JMA covered 0.33% of the national land area, it accommodates as much as 12% of Indonesia`s total population (Goldblum *et al*, 2000; Firman, 2009). Urbanization has significantly influence on spatial and environment development in Indonesia, particularly in urban space. Urban development in Indonesia particularly in Java island can be recognized by rapid changes of the land use and its urban centers, as well as by conversion vegetation area to built-up area. These processes can be seen clearly in large cities were mostly standing on Java island, such as Jakarta Metropolitan Area (JMA), Surabaya, Bandung, and Semarang.

Jakarta as the main city in Indonesia has faced several environmental problems related to intensive urbanization there. Jakarta has experience of flood disaster that occurs almost in every year and inundating almost whole over Jakarta city. 40% area in Jakarta is in the lowlands and influenced by tidal, crossed by 13 rivers, flooding will frequently occur when heavy rainfall is coming (Kagabu et al, 2011; Steinberg, 2007). However, the flooding in Jakarta is not only caused by natural disaster, but also human interface. Lack of carrying capacity of flood control infrastructures, reduction of the capacity of existing systems in uncontrolled garbage dumping, reduction of rain water

absorption due to urbanization and deforestation is the main influenced by flooding in Jakarta (Steinberg, 2007).

1. 2. Literature review

Climatic risk relating urbanization

A climatic effect caused by the urbanization is to be paid attention recently for more than half of the world are living in the urban area which expect to increase. Urban heat island (UHI) is the common phenomena that can be found during the specific heat difference of urban and rural area. UHI effect has been linked to some disease caused by the urban heat environment and socio-demographic aspect. The UHI effect has proven to be deadly in heat waves in Chicago in 1995 and Paris in 2003, where thousands of people died of heat-related illness (Aboff et al, 2010). Heat stroke caused by extreme heat wave is a severe illness clinically defined as core body temperature $\geq$ 40.6°C ($\geq$105 °F), accompanied by hot, dry skin and central nervous system abnormalities, such as delirium, convulsions, or coma (Luber and McGeehin, 2008). Urbanization can treat such as ecological safety regarding to the horizontal land expansion and reducing vegetation space. Lack of vegetation space means the impervious surfaces are increasing which is altering how solar radiation is reflected, emitted, and absorbed. The lost of vegetation space is causing soil moisture and evapotranspiration decrease, resulting air temperature increase.

Environmental damage related to climatic risk also happens in Jakarta city as the research area. Dengue hemorrhagic fever (DHF) is one of the vector-based disease which are very sensitive to the climate variation (number of rainy days, solar radiation, humidity) in tropical country such as Indonesia, Thailand, Philippines, and Bangladesh (Dulay et al, 2013; Zubaidah, 2013; Tipayamongkholgul and Lisakulruk, 2011, and Karim et al, 2012). World Health Organization (WHO) stated that social and environment factors including urbanization (lack of health services for poor families), climatic variation may affect transmission, as dengue mosquitoes reproduce more quickly and bite more frequently at higher temperatures (The World Health Organization, 2003).

Surface temperature (T_S) in in remote sensing satellite

Urban areas which covered by impervious surfaces as anthropogenic features would lead to increase in the volume, duration, and intensity of urban runoff (Voogt and Oke, 2003; Weng et al, 2004). In addition, urban surfaces would modify sensible and latent heat flux within the urban canopy and boundary layer. There are three variables which were identified to be closely correlated to local temperature variation: Land Surface Temperature (LST; T_S), vegetation cover, and impervious surface percentage. The impact of urbanization on the thermal environment is generally known as urban heat effect which generates near the ground surfaces and gives result in LST anomalies (Voogt and Oke, 2003; Kataoka et al, 2009; Lazzarini et al, 2013).

Thermal infra-red remote sensing data were commonly known as a source to determine the T_S from space. T_S originates from the balance between absorbed solar radiation and losses through sensible heat and latent heat fluxes as well as radiant emissions which governed by moisture content, surface type, wind velocity and emissivity. It was assumed that variability of T_S affects T_a particularly in clear-sky days (Voogt and Oke, 2003). T_S remote sensing can contribute to provide large scale earth surface distribution temperature data and also about isolated areas, meanwhile it has limitation to calculate detail information of temperature in earth surfaces.

The LST (T_S) products that used in this research are derived from Moderate Resolution Imaging Spectroradiometer (MODIS) and Landsat images. The MODIS LST (T_S) is derived from two thermal infra red (TIR) band channels, 31 (10.78 – 11.28 µm) and 31 (11.77 – 12.27 µm). The MODIS sensor is aboard the Terra and Aqua platform. LST Terra data is available during day and night time around 10.30 – 12.00 a.m and p.m local time and LST Aqua around 1.00 – 3.00 a.m and p.m. We used both data to cover the research in dry season period (July – October, 2012). Regarding the process to estimate air temperature from LST (T_S) products, the latest MODIS LST version, v005, was downloaded from the MODIS website. This product aims at retrieving LST with an error lower than 1°C (±0.7°C standard deviation) in the range of - 10 to 50°C, assuming that surface emmisivity is known (Benali et al, 2012). To quantitatively measure LST (T_S) and estimate air temperature in the past (1989 and 2006), we selected Landsat 7 thermal data. It has spatial resolution of 30 m in bands 1–

5 and 7 have a spatial resolution of 30 m, and the thermal infrared band (band6) has a 60 m for Landsat 7 images.

Air temperature (T_a)

Traditionally, T_a measured at standard meteorological station in 1.5 – 2 m height above the ground and it is a key to describe energy and water cycles of the earth-atmosphere system. The spatiotemporal patterns of near- surface air temperature are complex because T_a is strongly determined by surface properties that vary in both space and time (Prihodko, and Goward, 1997). The earth-atmosphere system is balanced by the absorption of incoming solar radiation, in the shortwave part of the light spectrum, and the emission of infrared long wave radiation and the sensible and latent heat loss fluxes (Prihodko and Goward, 1997; Jin and Dickinson, 2010.; Benali et al, 2012). These processes are the main component of the T_a daily cycle. The landscape changing in urban area affects the environment and it can have a significant impact in the air temperature (T_a) as shown by both long-term analyses of ground-based measurements and analysis of satellite data.

LST (T_S) and air temperature (T_a) have close correlation, but both of them have different physical meanings, magnitudes, measurement technique, response to atmospheric condition and diurnal phase (Jin and Dickinson, 2010; Benali et al, 2012). T_a information is not provided by satellite because the gap between LST (T_S) and T_a rate can very greatly different in diurnal cycle, and patterns are influenced seasonally through variation in the day and night time lengths (Benali et al, 2012). During daytime T_a is lower than LST (T_S) and at night time is opposite. In daytime, the energy of outgoing long wave-radiation driven by solar insolation is dominant, so LST (T_S) can be detected by satellite. On the other hand, during nighttime, lack of solar insolation effect on outgoing thermal infrared and reduce the signal of LST (T_S) compared with T_a.

Current Research on urban thermal environment

Previous studies have revealed many research on urban remote sensing particularly using LST (T_S) as an indicator of heat island (Tursilowati et al, 2012; Rizwan et al,

2008; Hung et al, 2006). Other study are investigate the relationship between LST (T_S) and vegetation cover (Weng et al, 2004; Chen et al, 2006), and impervious surfaces in urban area (Yuan and Bauer, 2007; Xu, 2010; Weng, 2012). However, not much study investigate LST (T_S) product to calculate air temperature to detect urbanization. Commonly, moderate and low spatial scale of LST (T_S) satellite products are used to reveal T_a from satellite approach, however, the effectiveness and sensitivity of each type is unclear.

1. 3. Study area

Indonesia capital city, Jakarta, become the study area of this research. Daerah Khusus Ibukota (DKI) Jakarta or Special Capital Territory of Jakarta, as known as Jakarta is the biggest city in Indonesia as an area of 662 km^2. The Jakarta urban area with the core is in Jakarta city, now become extended in surrounding cities. In 2011, the world counted 23 megacities of at least 10 million inhabitants accounting for 9.9% cent of the world urban population. In 2006, the population density in the capital of Indonesia, Jakarta, is 13,526 inhabitants/km^2, which is comparable with several other major cities in the world, such as Tokyo (13,333 inhabitants/km^2) and New York (10,292 inhabitants/km^2), respectively.

Table 1.1 Demographic in Jakarta

	Jakarta	**Metropolitan Area**	**Republic of Indonesia**
Land area (km^2)	662	7,297	1,919,440
Population	9,588,198	28,019,545	238,000,000
Population density/km^2	14,464	4,383.53	134

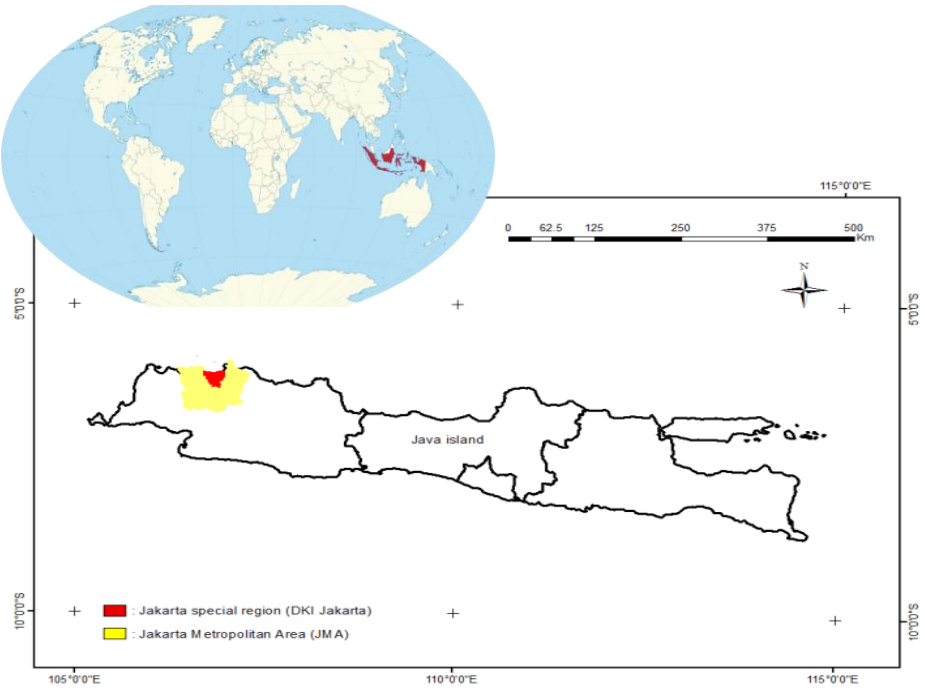

Figure 1. 1 The Greater Jakarta

Jakarta expanded from 180 square kilometers in 1960 to a fully urbanized megapolis in the 2000s. Today, as mega city, Jakarta`s nucleus area has spatially and economically expanded beyond its original fringes and has been integrated with four other proximate cities, namely Jakarta Metropolitan Area (JMA). In Jakarta there are existence of some 1.3 million private cars, 2.6 million motorcycles and 800,000 buses and lorries (2002 data representing a 10-fold increase since 1985) on Jakarta's roads illustrate the amount of traffic that is circulating in Jakarta, a city which has a rather limited road space available (Steinberg, 2007).

1. 4. Objectives

The main goal of this research is detecting urbanization effect in Jakarta city from surface temperature approach. The specific objectives are as follows:

1. To assess land use distribution as an impact of urban extension in Jakarta city.
2. To assess the thermal environment during 1990s – 2000s in order to obtain land surface temperature in urban area using satellite imageries in Jakarta city.

3. Air temperature estimation in urban area by combining ground base meteorological data and surface temperature from remote sensing data to detect urbanization effect in Jakarta city.
4. To investigate urban development in urban area based on thermal environment condition in Jakarta city.

1. 5. Dissertation structure

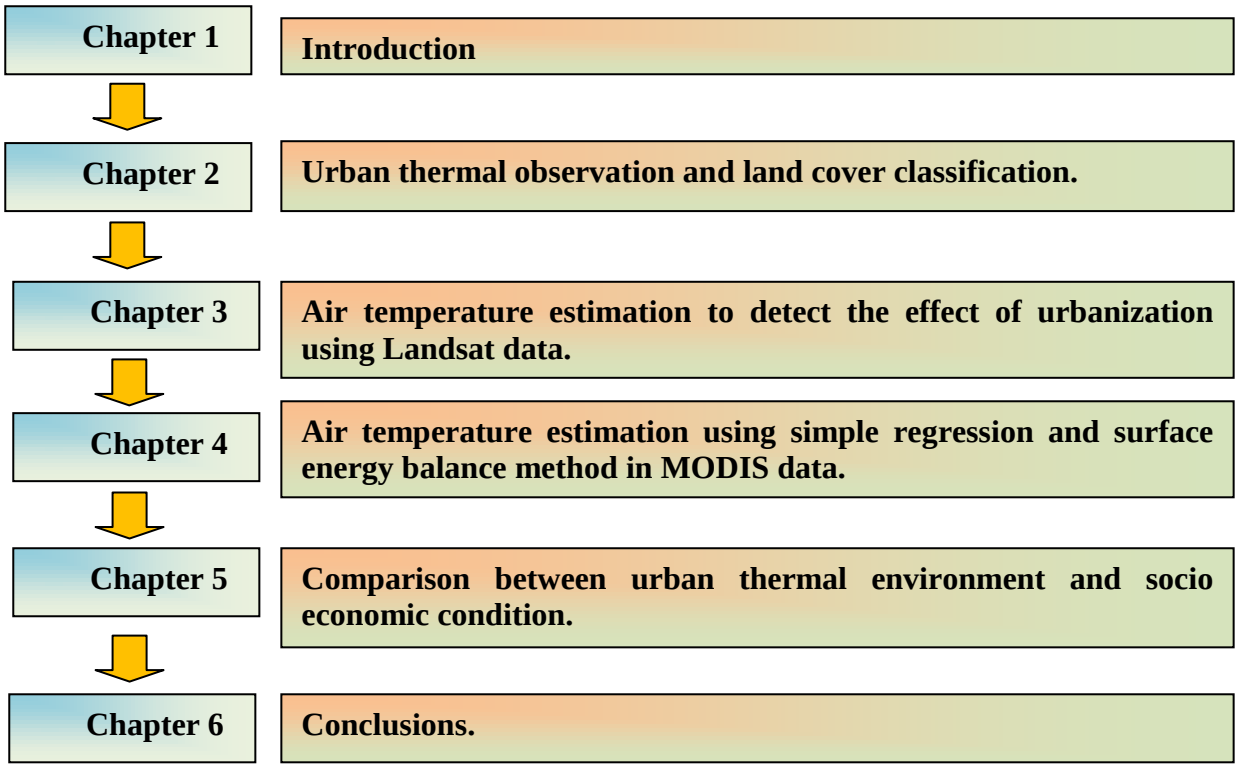

Figure. 1.2 Dissertation structure

References

UN-ESCAPE. 2011. Statistical Yearbook for Asia and The Pacific. pp. 7–8.

National Aeronautics and Space Administration. 2011. Landsat 7 Science Data Users Handbook. p. 120.

Aboff, Amelia., et al. 2010. Trees and the urban heat island effect : a case study for providence rhode island. Center for Environmental Studies, Brown University.

Benali, A., Carvalho, A.C., Nunes, J.P., Carvalhais, N., and Santos, A. Estimating air surface temperature in Portugal using MODIS LST data. *Remote Sensing of Environment*, 124 (2012), pp. 108–121.

Chen, Ling-Xiao, Zhao, Mei-Hong, Li, Xiang-Ping, Yin, Yong-Zhi. Remote sensing image-based analysis of the relationship between urban heat island and land use/cover changes. *Remote Sensing of Environment* 104 (2006) 133–146.

Dulay, S. Velora, Aubrey., Bautista, R. Jing., and Teves, G. Franco. Climate Change and Incidence of Dengue Fever (DF) and Dengue Hemorrhagic Fever (DHF) in Iligan City, Lanao del Norte, Philippines . *International Research Journal of Biological Sciences* Vol. 2(7), 37-41, July (2013).

Firman, Tommy. The continuity and change in mega-urbanization in Indonesia: A survey of Jakarta–Bandung Region (JBR) development. Habitat International 33 (2009) 327–339.

Goldblum, C., and Wong, T.. Growth, crisis and spatial change: a study of haphazard urbanization in Jakarta, Indonesia. *Land Use Policy*, 17 (2000), pp. 29–37.

Jin, M., and Dickinson, E.R. Land surface skin temperature climatology: benefitting from the strengths of satellite observations. *Environmental Research Letters*, 5 (2010) 044004 (13 pp).

Kagabu, Makoto; Shimada, Jun; Delinom, Robert; Tsijimura, Maki; and Taniguchi, Makoto. Groundwater flow system under a rapidly urbanizing coastal city as determined by hydrogeochemistry. *Journal of Asian Earth Sciences* 40 (2011) 226–239.

Kataoka, K., Matsumoto, F., Ichinose, T., and Taniguchi, M. Urban warming trends in several large Asian cities over the last 100 years. *Science of the Total Environment*, 407 (2009), pp. 3112– 3119.

Karim, Nazmul., Munsi, Ullah, Saif., Anwar, Nazneen, and Alam, Shah. Climatic factors influencing dengue cases in Dhaka city: a model for dengue prediction. *Indian J Med Res* 136, July 2012, pp 32-39.

Lazzarini, Michele., Marpu, P.R., and Ghedira, Hosni. Temperature-land cover interactions: The inversion of urban heat island phenomenon in desert city areas. *Remote Sensing Environment 130 (2013) 136 – 152.*

Luber, George, and McGeehin, Michael. Climate Change and Extreme Heat Events. *American Journal of Preventive Medicine* 2008;35(5):429 –435.

Prihodko, Lara., and Goward, N. Samuel. Estimation of air temperature from remotely sensed surface observations. *Remote Sensing and Environment* 60: 335 – 346 (1997).

Steinberg, Florian. Jakarta: Environmental problems and sustainability. *Habitat International* 31 (2007) 354–365.

Tipayamongkholgul, Mathuros, and Lisakulruk, Sunisa. Socio-geographical factors in vulnerability to dengue in Thai villages: a spatial regression analysis. *Geospatial Health* 5(2), 2011, pp. 191-198.

The World Health Organization, 2003. Climate Change and Human Health : Risks and Responses.

Tursilowati, Laras., Tetuko, Josaphat., Kuze, Hiroaki., and Adiningsih, S. E. Relationship between Urban Heat Island Phenomenon and Land Use/Land Cover Changes in Jakarta – Indonesia. *Journal of Emerging Trends in Engineering and Applied Sciences*, 3 (4): 645 – 653 (2012).

Voogt, J.A, and Oke, T.R. Thermal remote sensing of urban climates. *Remote Sensing of Environment*, 86 (2003) 370–384.

Weng, Qihao. Remote sensing of impervious surfaces in the urban areas: Requirements, methods, and trends. *Remote Sensing of Environment* 117 (2012) 34–49.

Weng, Qiahao., Lu, Dangsheng, and Schubring, Jacqelyn. Estimation of land surface temperature–vegetation abundance relationship for urban heat island studies. *Remote Sensing of Environment* 89 (2004) 467–483.

Xu, Hanqiu. Analysis of impervious surface and its impact on urban heat environment using the normalized difference impervious surface index (NDSI). *Photogrametric Engineering and Remote Sensing* Vol. 76, No. 5, May 2010, pp. 557-565.

Yuan, Fei, and Bauer, E. marvin. Comparison of impervious surface area and normalized difference vegetation index as indicators of surface urban heat island effects in Landsat imagery. *Remote Sensing of Environment* 106 (2007) 375–386.

Zubaidah, Tien. Impacts of Climate Change on Dengue Haemorrhagic Fever Cases in Banjarbaru Municipal, South Kalimantan During the Year 2005-2010. *Indonesian Journal of Wetlands Environmental Management* Volume 1, Number 1, September 2013.

CHAPTER 2

URBAN THERMAL OBSERVATION AND LAND COVER CLASSIFICATION

2. 1. Introduction

The development activities in the fringe of JMA have been dominated by low density, non–contiguous and land intensive residential area. They have scattered across the regions and consumed large area of vegetation space including agricultural land. As a result the predominantly agricultural activities in the fringe area were transformed into industrial and service based activities (Firman, 1997). In term of its spatial pattern, based on some urban spatial indicators defines the development practice in the fringe of Jakarta as sprawl (Bertaud, 2001). Rapid development will affect the landscape, which, if it occurs in rural areas will change from vegetation area (non built up area) to built up area. The number of megacities has been increasing in Asia. A megacity is defined as a city with a population larger than 10 million. With the rapid population increase, the urban area also expanded rapidly within the past several decades, which may have strongly affected the urban land features. Jakarta's urban fringe is growing much faster than the city itself. The change of land cover is suspected as the one which influence of thermal increases. In order to understand the distribution and present condition of those parameters, field observation was carried on in Jakarta city in September – October, 2012.

2. 2. Observation in Jakarta

There were two kinds measurement during observation period. In fix point measurement, we install the equipment in eight locations. Two equipments is in inside Jakarta (Kramatjati and Cijantung), and six equipments is in Jakarta fringe area (Bekasi, Bogor, Depok, and Tangerang). To measure the thermal environment in Jakarta urban area, we used OPTEX MI-710 as infrared thermometer, HOBO Pro v2 U23-002 as thermo hygrometer was set in 1.5 m height, and Mistral Instruments WDL-01 as aerovane was set in 2 m height in each point locations.

Figure 2. 1 Fix point equipments installation. ⃠ is not use.

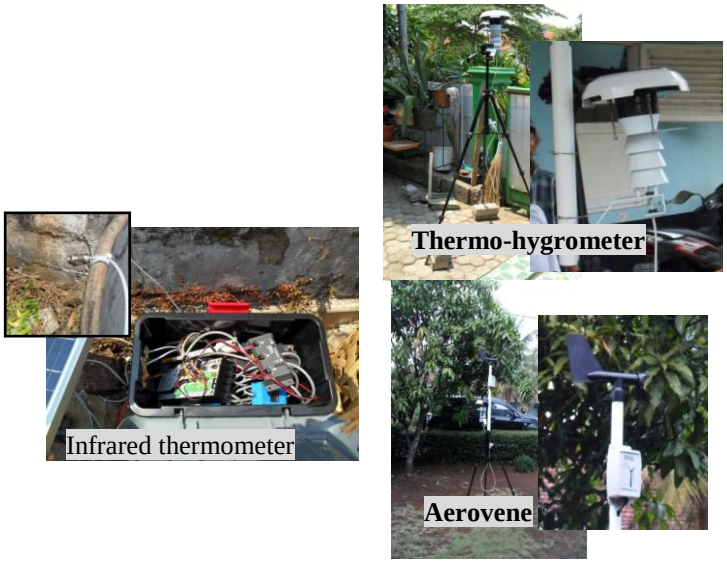

Figure 2. 2 Observation equipments at fix point

Mobile measurement was conducted to validate the surface temperature from remote sensing satellite and verify the land cover in Jakarta urban area. We selected 10 a.m – 12 a.m at local time as the same period with satellite overpass to carry out the mobile measurement. We used Fluke 568 as the portable infrared thermometer and T&D Corporation TR-77Ui as Portable thermo-hygrometer.

Portable thermo-hygrometer Portable infrared thermometer

Figure 2. 3 Mobile measurement equipments

2. 3. Land cover classification

The objective of image classification is to categorize pixels in an image into land cover classes or themes (Lillesand., Kiefer., and Chipman, 2007). To classify the land cover in study area, Landsat TM in 1989 and Landsat ETM+ in 2006 was used. To execute the land cover classification process, supervised classification technique is chosen. There are three steps to proceed supervise classification in remote sensing image, (1) identify representative training area for each land cover types, (2) categorize

each pixel into land cover class, (3) digitalize the result as thematic map (Lillesand., Kiefer., and Chipman, 2007).

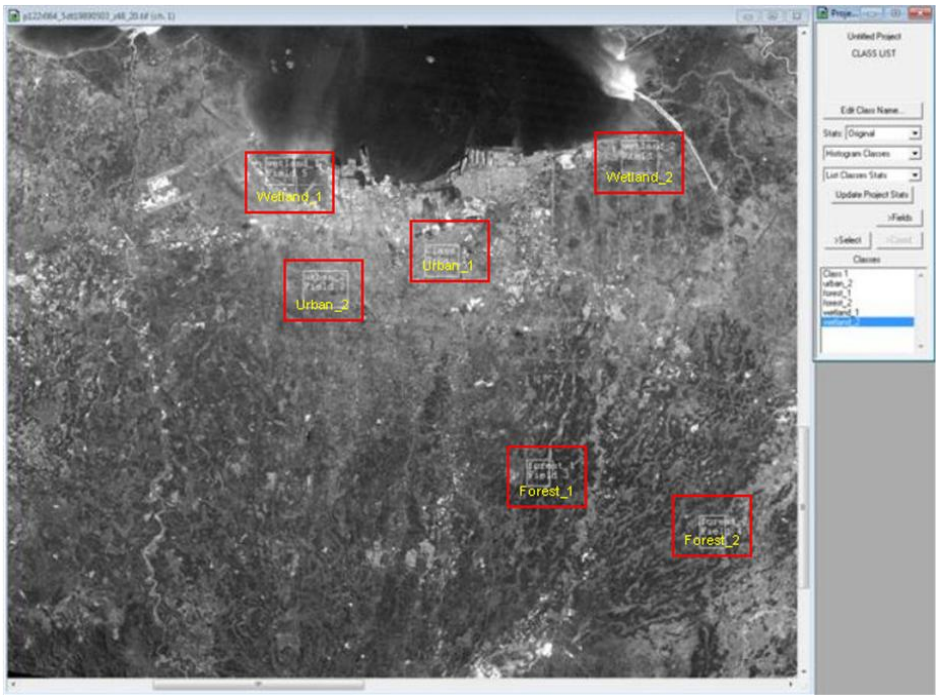

Figure 2. 4 Land cover classification step using MultiSpec software. ☐ is the training area in image scene.

We choose maximum likelihood classifier to proceed this step. Four land cover types were classed and in each type we made 14-30 training areas depend on the land cover large area. The overall class performance is 75% and Kappa statistic for this step is 85% which that mean this result is representative enough for present land cover distribution.

2. 4. Result and discussion

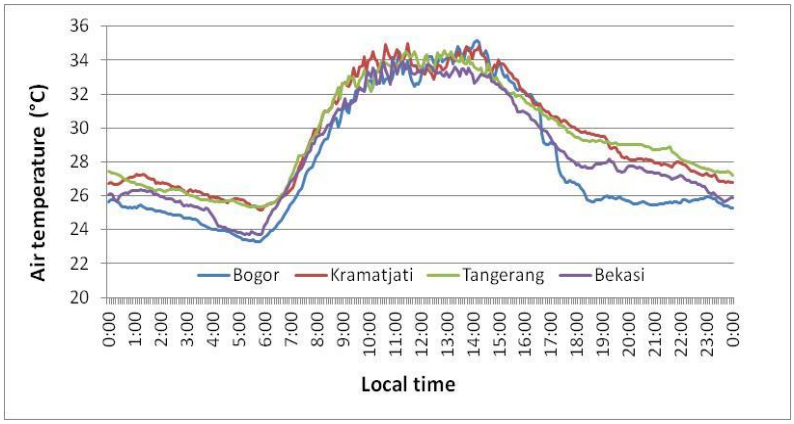

Figure 2. 5 Air temperature in fix observation point in Jakarta city and suburban area

Figure 2. 5 shows the 24 hours air temperature and relative in Jakarta as the core city and its fringe area (Bogor, Tangerang, and Bekasi) on 29 - 30 September 2012 (dry season). As the urbanized area, Jakarta relatively has high temperature compare to other cities. At the midnight, whole cities have low temperature, and the lowest is Bogor. Bogor is located in the southern part of Jakarta and gets less influence of sea breeze from the Java seas (northern Jakarta). Opposite with Bogor site, Tangerang which is located relatively close to the sea get more influence in sea breeze. In the daytime, the temperature reached the peak level and cooling down in around 15 p.m. Here, Jakarta and Tangerang (urban) are kept on their higher temperature than Bogor and Bekasi (suburban). Urban area much slower in cooling and has stronger heat than suburban area at the nighttime, this can be identified as heat island effect.

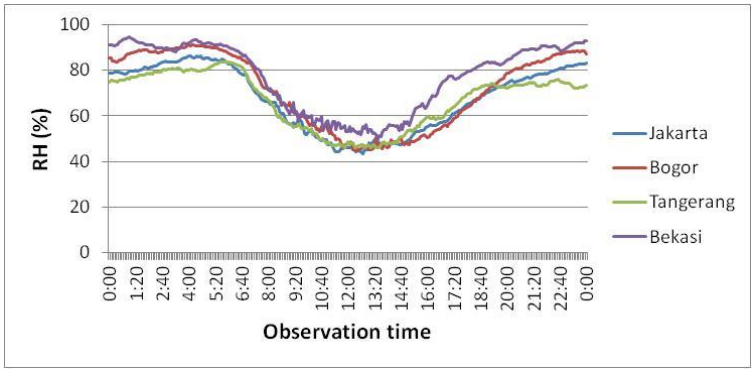

Figure 2. 6 Relative humidity in fix observation point in Jakarta city and suburban area.

Lower relative humidity (RH) was occurred during the night time to early morning in the high urbanized area caused by the low vegetation evapotranspiration; while in the suburban area is higher. In the daytime, the relative humidity in whole area was decreasing caused by the high intensity of solar radiation and the sea breeze (Java sea) which carried water vapor is penetrate to the urban center. In the early evening to the midnight RH was generally increase because the solar radiation and sea breeze is become weak, but in some specific area which sited in coastal area (Tangerang and Bekasi) it seems to be high than the others. At the midnight time, RH was high in the suburban (Bogor) caused by the mountain breeze which carried water vapor was penetrate this area.

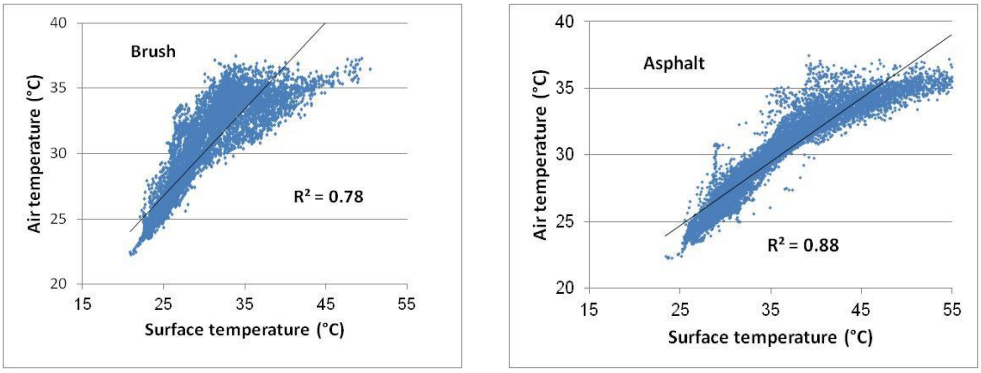

Figure 2.7 Scatter diagram between air temperature (T_a) – surface temperature (LST;T_S) in Jakarta.

Figure 2.7 shows the comparison between T_a and LST (T_S) in Jakarta`s observation site. High coefficient correlation (R^2) was produced in two surface types, brush and asphalt. To understand urbanization in Jakarta city and the spatial distribution of land use types, we were classifying it by using Landsat time series data which downloaded from http://glcf.umd.edu/data/. Land- use maps were governed using supervised classification based on the Maximum Likehood algorithm in Multyspec software. Land-use types were classified including vegetation, urban/built-up, brush, and water body. Landsat TM in 1989 and Landsat 7 ETM+ in 2006 were selected to produce time series land-use maps.

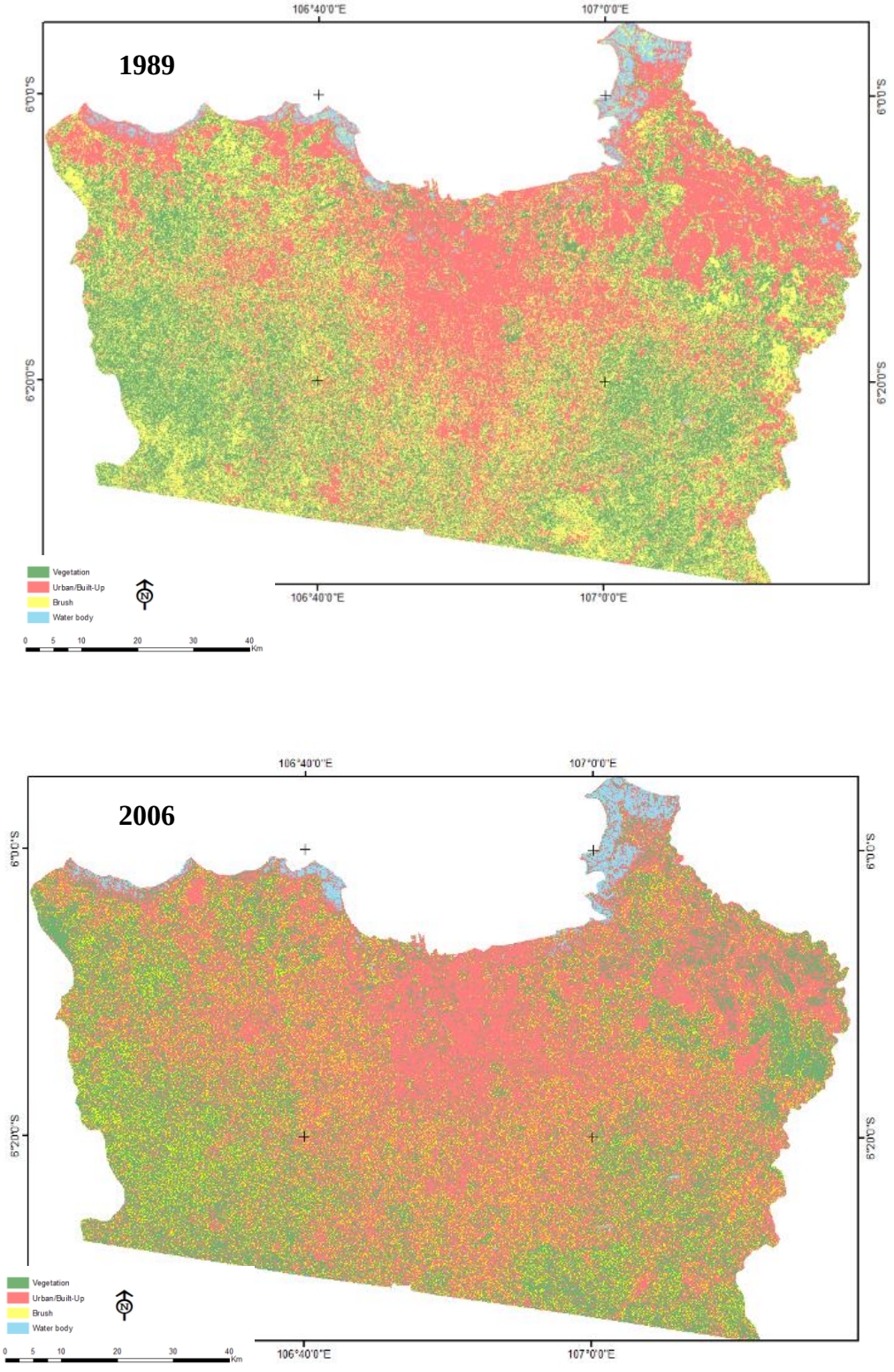

Figure 2. 8 Land cover classification in 1989 and 2006

Table 2.1 Land cover classification

Land cover	Area (sq. km)	
	1989	2006
Brush	1463	646
Vegetation	1536	676
Urban/Built-Up	1692	3369
Water body	85	85
Total	**4776**	

Figure 2.1 shows the land cover classification in Jakarta urbanized area in 1989 and 2006. The urbanized area was detected and recognized by the distribution of urban/built-up area surfaces in 2006. Table 2.1 shown that urban/built-up area was double increased in 2006 and it was distributed spread over from the center urban areas.

Table 2.2 Land cover area in DKI Jakarta and West Java Province by Statistic Bureau

Land cover	Area (sq. km)			
	Jakarta		West Java	
	1989	2006	1989	2006
Built up	509	528	7,384	12,220
Non built up	141	122	27,080	22,244

: Built up : Non built up

Table 2.2 shows the land cover classification in Jakarta city in 1989 and 2006 from DKI Jakarta and West Java province statistic bureau. During a decade, built up area has increasing while non-built up area has been decreased. This result is similar as detected in satellite remote sensing classification.

2. 5. Summary

To understand the thermal environment in the Jakarta urban area, we observed and installed fixed-point temperature equipments from dry to pre-monsoon season (16 September to 18 October) in 2012. Strong thermal environment was created in urban centers where high concentration urban/built-up area was governed. At the night time, urban and suburban area have large difference in T_a, while in the early morning it become smaller. This observation data indicated that the temperature was followed by

the change of surface feature. The urbanized area (northern part) faced low relative humidity during the day caused by low vegetation evapotranspiration and sea breeze penetration, while in the midnight; suburban area (southern part) has a higher relative humidity caused by the water vapor from the mountain breeze.

The high urbanized area is detected from the land cover distribution in 1989 and 2006 from the satellite image. The built-up area is not only concentrated in the urban center, but also in the southern part area. These results indicate that urbanization in Jakarta city is become wider. Through the thermal observation data, briefly urban thermal condition in Jakarta urban area was defined. These observation data also can be used to validate to validate physically based meteorological models and satellite remote sensing, and finally to analyze sustainable urban development in Jakarta.

References

Bertaud, Alain. The Spatial Organization of Cities: Deliberate Outcome or Unforeseen Consequence? Working Paper 2004-01. Institute of Urban and Regional Development University of California at Berkeley.

Firman, Tommy. The continuity and change in mega-urbanization in Indonesia: A survey of Jakarta–Bandung Region (JBR) development. *Habitat International* 33 (2009) 327–339.

Firman, T. Land Conversion and Urban Development in the Northern Region of West Java, Indonesia. *Urban Studies* 34(7): 1027-1046 (1997).

Lillesand, M. Thomas., Kiefer, W. Ralph., and Chipman, W. Jonathan. Remote Sensing and Image Interpretation (6th edition). John Wiley & Sons, 2007.

Steinberg, Florian. Jakarta: Environmental problems and sustainability. *Habitat International* 31 (2007) 354–365.

Tokairin, Takayuki., Sofyan, Asep., and Kitada, Toshihiro. Effect of land use changes on local meteorological conditions in Jakarta, Indonesia: toward the evaluation of the thermal environment of megacities in Asia. *International Journal of Climatology* 30: 1931–1941 (2010).

Tursilowati, Laras., Tetuko, Josaphat., Kuze, Hiroaki., and Adiningsih, S. E. Relationship between Urban Heat Island Phenomenon and Land Use/Land Cover Changes in Jakarta – Indonesia. *Journal of Emerging Trends in Engineering and Applied Sciences*, 3 (4): 645 – 653.

CHAPTER 3

AIR TEMPERATURE ESTIMATION FROM SATELLITE REMOTE SENSING TO DETECT THE EFFECT OF URBANIZATION USING LANDSAT DATA

3. 1. Introduction

Urbanization is defined as higher proportion of urban population, is growing rapidly in Indonesia, particularly in large cities such as Jakarta. Java, overwhelmingly the most populated island, is 65% urbanized with an urban population of 78 million. In 2025, the country is expected to be 61% urbanized with an urban population of 167 million people (The World Bank, 2002). Jakarta is the dominant city, capital, and an extended urban region of approximately 17 million people.

Numerous studies have indicated that urban expansion has caused localized increases in the air temperature (T_a) as shown by both long-term analysis of ground-based measurements (Goldblum and Wong, 2000; Kataoka et al, 2000) and analysis of satellite data (Jiang, and Tian, 2007; Rizwan, Leung, and Liu, 2008; Tursilowati et al., 2012). Heat islands degrade residential environments and increase the risk of heat-related illnesses and dengue; thus, temperature monitoring is an important issue. However, monitoring heat-island temperatures has proven to be difficult, requiring a dense network of observation sites to record T_a in various locales. As such, several studies have investigated the use of the land surface temperature (LST; T_S) readings derived from satellite data as an indicator of heat islands.

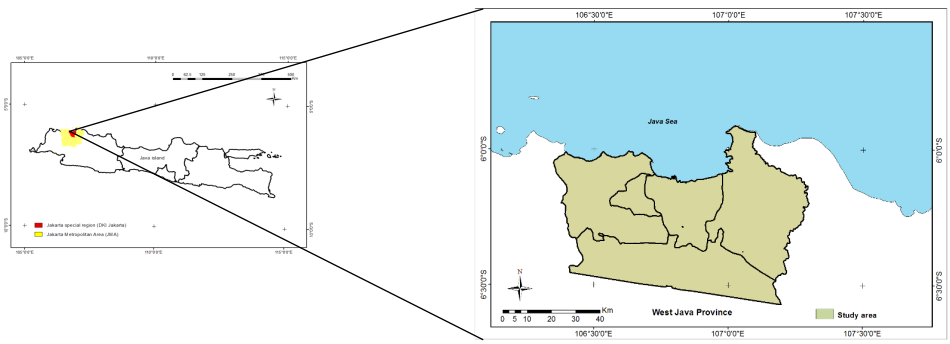

Figure 3. 1. Study area in Jakarta, Indonesia, urban area

Thermal infra-red remote sensing data was commonly known as a source to determine the T_S from space. T_S originates from the balance between absorbed solar radiation and losses through sensible heat and latent heat fluxes as well as radiant emissions which governed by moisture content, surface type, wind velocity and emissivity. It was assumed that variability of the T_S affects T_a particularly in clear-sky days (Voogt and Oke, 2003). The objective of our study is to demonstrate the feasibility of Landsat T_S product as a source for calculating spatial distribution of T_a to detect urbanization effect in Jakarta city.

3. 2. Air temperature (T_a) trends from the 1950s to 2010 in Jakarta

The daily average T_a time series was provided by the National Climatic Data Center (NCDC). Two stations were selected for the comparison of urban (Jakarta) and suburban (Bogor) areas. T_a, the near-surface air temperature, was measured 1.5–2 m above the ground, coinciding with weather station readings. Halim Perdanakusuma Airport or Jakarta Airport (the urban site) is located at S6°15'0", E106°54'0"; Atang Sanjaya (the suburban site) is located at S6°54'0", E106°32'60".

Figure 3. 2. Location of ground weather station in Bogor (suburban) and Jakarta (urban)

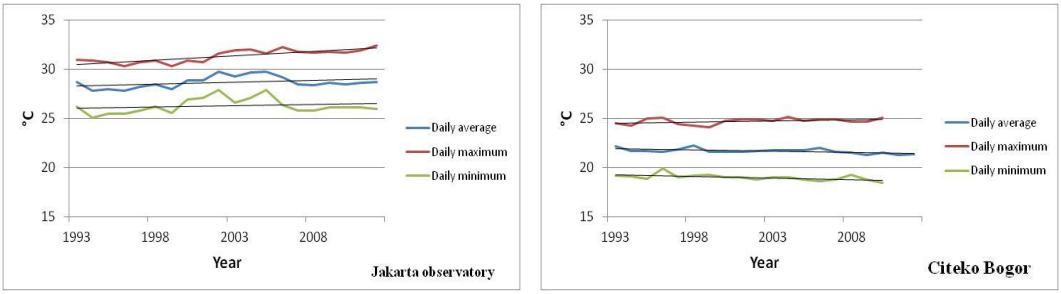

a **b**

Figure 3. 3. Time series of annual averaged daily minimum, maximum, and average temperature in (a) Jakarta (the urban area near Halim Perdanakusuma Airport) and (b) Bogor (the suburban area of Atang Sanjaya).

Figure 2. 2 shows the time series of 1-year averaged daily minimum, maximum, and average T_a in Jakarta (Halim Perdanakusuma Airport) and Bogor (Atang Sanjaya) during 1980–2010. The trend shows that the average and minimum T_a during the 1980s to 2000s increased in Jakarta, while the maximum T_a decreased. In comparison, the Bogor station showed a decreasing average, minimum, and maximum T_a over the same period. Table 3. 1 shows the 10-year average daily T_a obtained from the Jakarta and Bogor stations. The daily average T_a increased over the 10-year period in Jakarta, and remained unchanged over the same time period for Bogor.

Table 3. 1. Characteristics of air temperature (T_a) at selected stations.

Year	Average (°C)	
	Jakarta observation	Citeko Bogor
1991 - 2000	28.02	21.82
2001 - 2010	28.13	21.66

3. 3. Method

3. 3. 1. Land surface temperature (LST) retrieval method

Changes in the urban thermal environment resulting from urbanization should influence the LST, which is governed by land surface–atmosphere interactions and energy fluctuations between the atmosphere and the ground (Benali *et al*, 2012; Jim and Dickinson, 2010; Mildrexler, Zhao, and Running, 2005). LST can be used for remote-sensing thermal radiance measurements (Mildrexler, Zhao, and Running, 2005).

To determine the LST trends in Jakarta, daily Landsat time-series data were used. Ground-based measurements of LST were also obtained for comparison. Past Landsat data has thermal information offsets when it compared to present condition, then, to get actual absolute value ground-based LST measurement was needed.

Landsat thermal data using the thermal infrared (TIR) band can be used to determine the surface temperature (T_S) because the daytime satellite provides LST values that are much closer to the maximum daily temperature of the land surface, where the diurnal highest thermal response reflection occurs with respect to vegetation and dry surfaces (Mildrexler, Zhao, and Running, 2005; Coops, Duro, Wulder, and Han, 2007). In this research, Landsat TM/ETM series data, acquired in May 1989 and July 2006, were used to investigate the urban thermal environment. This time series was chosen due to the absence of clouds over Jakarta. The procedure used to retrieve T_S was based on the Landsat 7 Science Data Users Handbook (Landsat User Handbook, 2011).

The satellite image, *DN*, must first be converted to a spectral radiance value, *L*, as follows:

$$L = (\mathrm{LMAX} - \mathrm{LMIN})/255 \times \mathrm{DN} + \mathrm{LMIN}, \quad (1)$$

where *DN* is the digital number reading, and *LMAX*, *LMIN* are derived from the gain status indicated by the satellite image header file. The spectral radiance value is then converted into a brightness temperature for the satellite sensor (T_b) using Eq. (2):

$$\mathrm{T_b} = \frac{K_2}{\ln(\frac{K_1}{L} + 1)} \quad (2)$$

where T_b is the effective satellite temperature in absolute temperature, K_1 and K_2 are calibration constants for the Landsat TM/ETM+ system, and L is the spectral radiance in W m^{-2} sr^{-1}μm. K_1 was set to 607.76, and K_2 was set to 1260.56 (Landsat User Handbook, 2011). The brightness temperature was determined by applying blackbody principles. Surface emissivity was considered in the estimation of T_S for the targets

(Sobrino, Jimenez-Munoz, and Leonardo, 2003; Voogt and Oke, 2003; Tursilowati et al., 2012).

$$T_S = \frac{T_b}{1 + (\lambda \times T_b/\rho) ln\varepsilon} \quad (3)$$

where T_S indicates the LST in absolute temperature, λ is the wavelength of the radiance emitted (λ = 11.5 μm), ρ = (h × c) / σ = 1.438 ×10^{-2} (m K) , h is Planck`s constant (6.626 × 10^{-34} Js), c is the velocity of light (2.998 × 10^{8} m/s), σ is the Boltzmann constant (1.38 ×10^{-23} J/K), and ε is the composite emissivity. In this study, ε = 0.97 was used for the soil and vegetation (Sobrino, Jimenez-Munoz, and Leonardo, 2003).

3. 3. 2. Variations in LST data

Figures 3. 4 (a) and (b) show the spatial distribution of the LST in the Jakarta urban area, derived from Landsat TM data obtained on 3 May 1989 and from TM data on 5 July 2006. A comparison with ground-based measurements was used to validate the estimated T_S values. The observation was carried out during 18–26 September 2012 at the same local standard time (10:00) at 35 sample points and with one point for the ground control measurement, located in the central urban site.

(b) LST in 1989

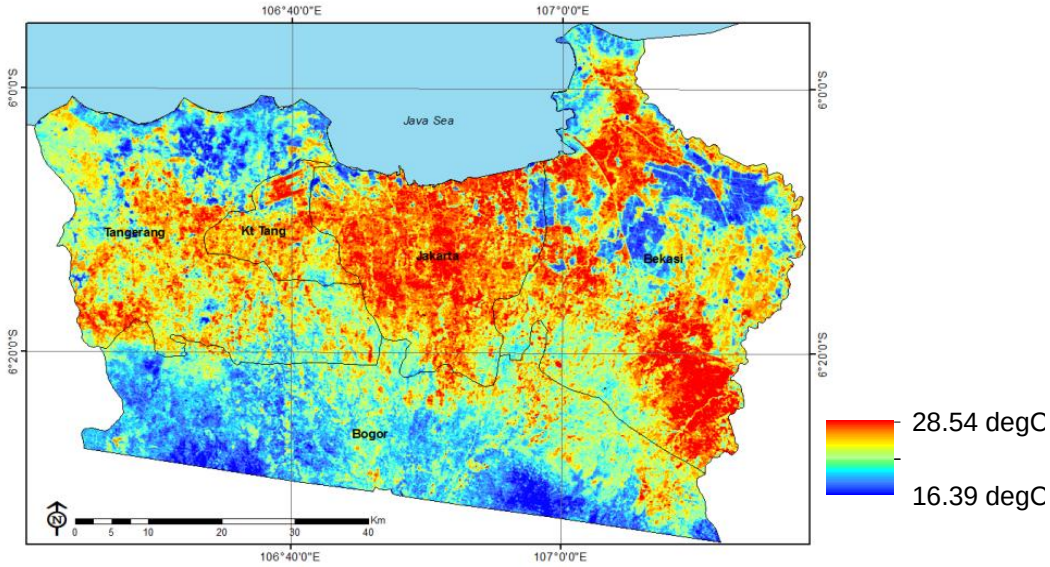

(a) LST in 2006

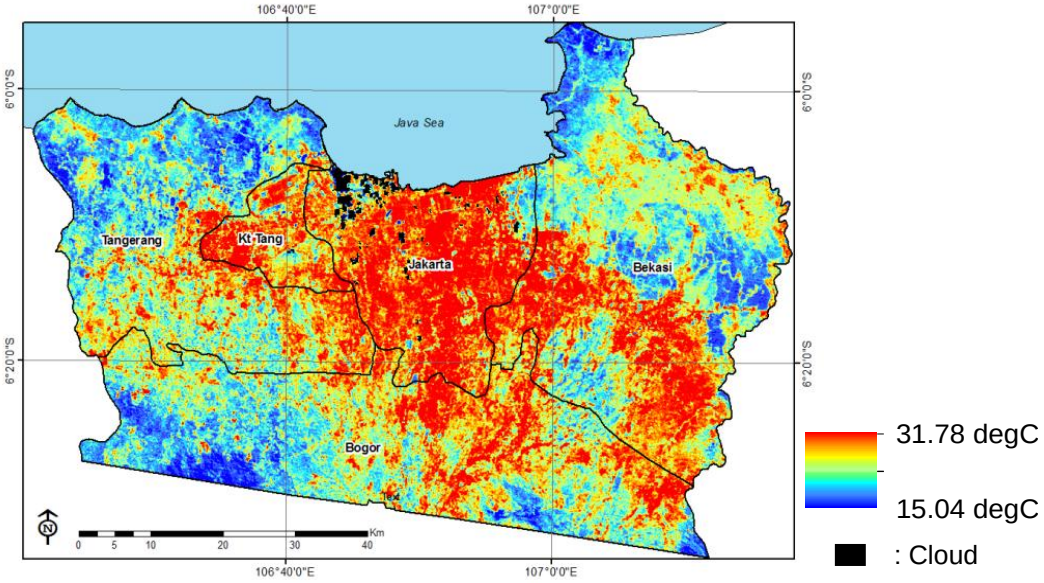

Figure 3. 4. Spatial distribution of surface temperature (T_S) a Jakarta urban area in (a) 1989 and (b) 2006.

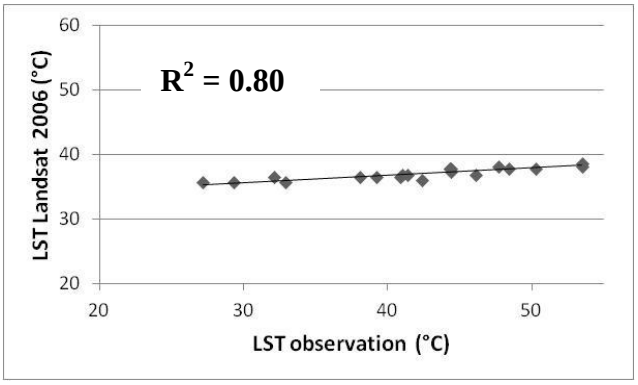

Figure 3. 5. Relationship between land-surface temperatures (LSTs) derived from satellite data and from ground-based measurements.

Strong correlation was observed between the estimated LST using Landsat data and ground measurements. The determination coefficient (R^2) was 0.8; thus, the LST

estimated by Landsat data provided a good representation of the actual LST in Jakarta (Mao, Qin, and Gong, 2005; Tursilowati et al., 2012). The LST was corrected based on regression relationships between the LST estimated by Landsat data and ground-based observations. The corrected LST distributions are shown in Fig 3.4. The comparison of results for 1989 and 2006 shows that the high-LST area had clearly expanded beyond the city center, as indicated by the 2006 data.

3. 4. Result and Discussion

3. 4. 1 Observed relationship between air temperature (T_a) and land surface temperature (LST)

To confirm the relationship between near-surface T_a and LST, ground-based measurements were carried out in Jakarta from 18 to 26 September 2012 at the same local standard time as that satellite images (10:00-12.00).

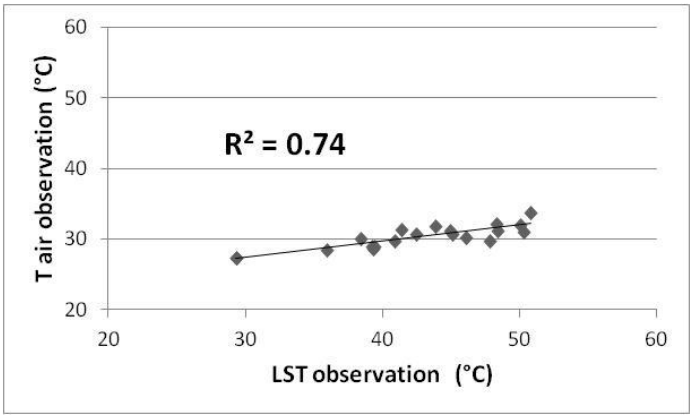

Figure 3. 6. Relationship between LST and air temperature (T_a) in ground-based observations.

Figure 3. 6 shows a scatter plot of the relationship between ground-based measurements of T_a and LST. The regression relationship was obtained by comparing T_a and LST. The determination coefficient (R^2) was 0.74, and it was also confirmed that the LST can be used as an indicator of T_a.

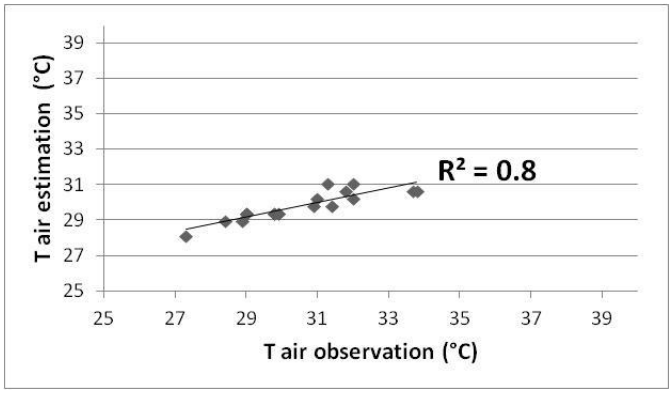

Figure 3. 7. Scatter plot of the relationship between T_a derived from satellite data and from ground-based measurements.

(b) Ta in 1989

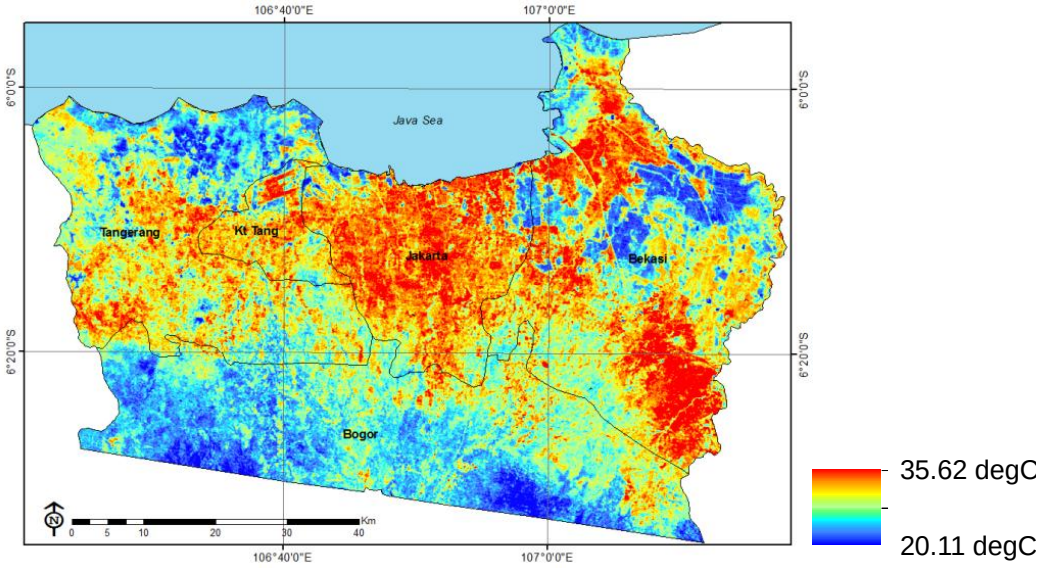

(a) Ta in 2006

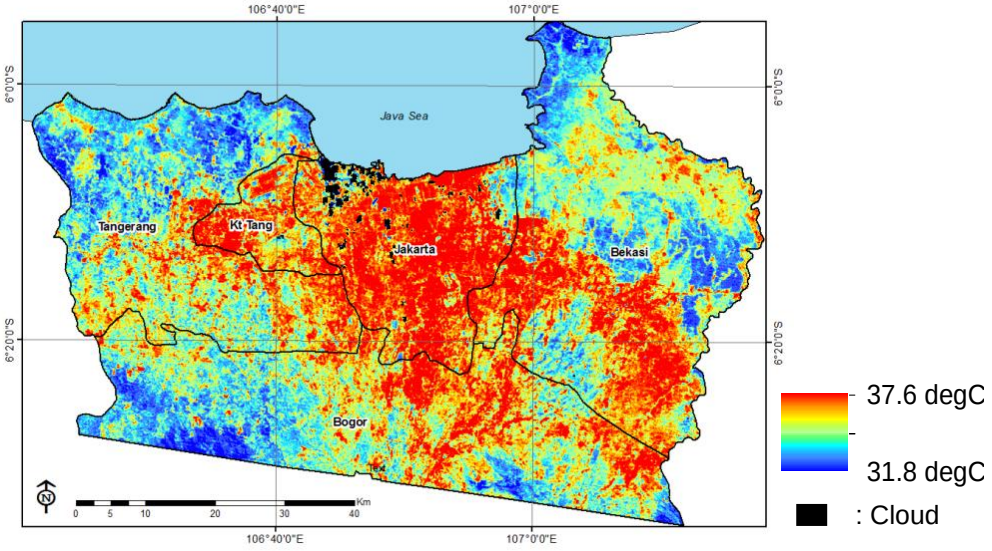

Figure 3. 8. Spatial distribution of air temperature (T_a) at Jakarta urban area in (a) 1989 and (b) 2006.

Figure 3.7 shows the relationship between T_a in ground-based measurements and that estimated by satellite-derived LST in 2006 to each corresponding pixel. The values show the deviations after being reduced from their initial values. A high R^2 coefficient (R^2 = 0.80) was determined in regression between T_a observation - T_a estimation 2006 with the RMSE is 1.80°C. To understand the T_a spatial distribution in 1989, the equation was applied on 1989`s satellite. Figure 3.8 shows the T_a spatial distribution in both years. On 1989 satellite, the minimum is 20.11 °C, maximum is 35.62 °C, and standard deviation is 5.93 °C. On 2006 satellite, the minimum is 31.8 °C, maximum is 37.6 °C, and standard deviation is 6.35 °C.

Table 3. 2. Minimum, maximum, and average of T_a and T_S in satellite data

Data	T_a (°C)		T_S (°C)	
	Minimum	Maximum	Minimum	Maximum
1989	20.11	35.62	16.39	28.54
2006	31.8	37.6	15.04	31.78

Nearly, all T_S were lower temperature in each data than the T_a. Differences between T_S and T_a tended to be larger in lower temperature. The large difference of average air temperature is also detected in each data satellite, it can be caused of air temperature is created in near surface of the earth and get large influence from surrounding area.

Table 3. 3. Comparison of air temperature (°C) between field measurement and Landsat 2006

Latitude	Longitude	Urban land cover	Landsat 2006 (°C)	Observation 2012 (°C)	Difference
6°22'07.7"	106°49'40.7"	Built up area	26.41	31.9	5.49
6°19'51.7"	106°49'46"	Built up area	26.41	31.6	5.19
6°21'18.6"	106°50'05.4"	Asphalt	25.99	29.7	3.71
6°27'46.5"	106°51'22.3"	Asphalt	25.14	27.6	2.46
6°12'31.7"	106°48'32.6"	Vegetation	26.83	32.9	6.07
6°10'46.4"	106°49'32.0"	Vegetation	26.83	32.1	5.27

Table 2. 3 is the comparison of air temperature between field measurement and Landsat 2006 in some corresponding pixels. 2006 data were chosen because those data is relatively close to the observation time. The difference between observation and satellite based varied locally by 2 – 6°C around noon. Our study is emphasizing on the affectivity of Landsat T_S to estimate T_a and neglected the land use or topographic aspects.

In this study, the application of Landsat imagery for estimating LST and T_a in Jakarta, Indonesia, using the observed relationship between T_S and T_a, was investigated. The results showed a strong correlation between Landsat T_S and ground-based T_S measurements in both years indicating that the Landsat T_S value provides a reliable representation of the actual LST. The range of determination coefficient (R^2) between T_a and LST in ground-based measurements was 0.74. Therefore, LST can be used as an indicator of T_a.

3. 5. Summary

LST product from Landsat 1989 and 2006 satellite was used in this research. T_a estimated from satellites tended to be higher than ground-based measurements, the use of satellite remote-sensing data can be used to overcome the spatial problem of

estimating T_a, particularly in areas with low station density, using satellite-based LST estimations and the ground-based relationship between LST and T_a.

References

Benali, A., Carvalho, A.C., Nunes, J.P., Carvalhais, N., and Santos, A. Estimating air surface temperature in Portugal using MODIS LST data. *Remote Sensing of Environment*, 124 (2012), pp. 108–121.

Coops, C.N., Duro, C.D., Wulder, A.M., and Han, T. Estimating afternoon MODIS land surface temperatures (LST) based on morning MODIS overpass, location, and elevation information for Canada. *International Journal of Remote Sensing*, 28 (2007), pp. 2391–2396.

Goldblum, C., and Wong, T.. Growth, crisis and spatial change: a study of haphazard urbanization in Jakarta, Indonesia. *Land Use Policy*, 17 (2000), pp. 29–37.

Jiang, J. and Tian, G. Analysis of the impact of land use/land cover change on land surface temperature with remote sensing. *Procedia Environmental Sciences*, 2 (2010), pp. 571–575.

Jin, M., and Dickinson, E.R. Land surface skin temperature climatology: benefitting from the strengths of satellite observations. *Environmental Research Letters*, 5 (2010) 044004 (13 pp).

Kataoka, K., Matsumoto, F., Ichinose, T., and Taniguchi, M. Urban warming trends in several large Asian cities over the last 100 years. *Science of the Total Environment*, 407 (2009), pp. 3112– 3119.

Mao, K., Qin, Z., and Gong, P. A practical split-window algorithm for retrieving land-surface temperature from MODIS data. *International Journal of Remote Sensing*, Vol. 26 (2005) No. 15, pp. 3181–3204.

Landsat 7 Science DataUsers Handbook. 2011. National Aeronautics and Space Administration. pp 53 – 120.

Mildrexler, J.D., Zhao, M., and Running, W.S. A global comparison between station air temperatures and MODIS land surface temperatures reveals the cooling role of forests. *Journal of Geophysical Research*, 116 (2011) GO3025.

Rizwan, A. Memon, D., Leung Y.C., and Liu, C. A review on the generation, determination and mitigation of urban heat island. *Journal of Environmental Sciences*, 20 (2008), pp. 120–128.

Sobrino, A.J., Jimenez-Munoz, C.J., and Leonardo, P. Surface temperature and water vapour retrieval from MODIS data. *International Journal of Remote Sensing*, Vol. 24 (2003), No. 24, 5161-5182.

The World Bank, 2002. Urbanization Dynamics and Policy Frameworks in Developing East Asia East Asia Infrastructure Department. http://siteresources.worldbank.org/INTEAPREGTOPURBDEV/Resources/Philippines-Urbanisation.pdfDownloaded, 25 March 2014.

Tursilowati, Laras., Tetuko, Josaphat., Kuze, Hiroaki., and Adiningsih, S. E. Relationship between Urban Heat Island Phenomenon and Land Use/Land Cover Changes in Jakarta – Indonesia. *Journal of Emerging Trends in Engineering and Applied Sciences*, 3 (4) 2012: 645 – 653.

Voogt, J.A, and Oke, T.R. Thermal remote sensing of urban climates. *Remote Sensing of Environment*, 86 (2003) 370–384.

Weng, Qiahao., Lu, Dangsheng, and Schubring, Jacqelyn. Estimation of land surface temperature–vegetation abundance relationship for urban heat island studies. *Remote Sensing of Environment* 89 (2004) 467–483.

Wubet, Tsehaye, Michael. Estimation of absolute surface temperature by satellite remote sensing. *Thesis of International Institute for Geo-information and Earth Observation, Enschede, The Netherland*. 2003. pp. 42 – 52.

CHAPTER 4

AIR TEMPERATURE ESTIMATION USING SIMPLE REGRESSION AND SURFACE ENERGY BALANCE METHOD IN MODIS

4. 1. Introduction

Climatology data can be governed for two kinds of surface temperatures: near-surface air temperature (T_a) and land surface temperature (LST). The air temperature near the earth`s surface is the most important variable wide range environmental spatial scale, and has many land surface processes. Air temperature (T_a) is measured at the 1.5 - 2 m height above the ground, and located in some ground base meteorological station has limitation in spatial scale (Prihodko and Goward, 1997). However, this kind data cannot reflect the spatial variation of T_a effectively especially in the location which difficult to observe (Wenbin, Aifeng, and Shaofeng, 2012). Different with climatic data retrieval in ground base weather station, remote sensing can obtained wider coverage area which observe land surface parameters such as surface temperature, and vegetation indices, etc (Wenbin, Aifeng, and Shaofeng, 2013). Land surface temperature (LST) is one of the important requirement parameter to estimate T_a for various satellite-based methods.

Surface temperatures (T_S) are set by land-atmosphere interactions and the energy fluxes between earth. It can be measured hand-held instrument or aircraft radiation thermometer as derived from upward long wave radiation based on the Stefan-Boltzman law or retrieved from thermal infrared satellite remote sensing observation after removing the noise caused by atmospheric effect on space craft radiances (Jin, Dickinson, 2010). As shown in chapter 3, several studies have been done to retrieve T_a from T_S remote sensing, first is based on regression technique by applied relationship between T_a and T_S (Kawashima et al, 2000; Colombi et al, 2007; Fu et al, 2011). Generally, this method is running well but has small sensitivity when comparing with T_a observation.

Another method is by assumed vegetation temperature by using vegetation indices such as Normalize Difference Vegetation Index (NDVI) (Prihodko, and Howard, 1997; Sandholt et al, 2002; Stisen et al, 2007; Wenbin et al, 2013). The average air temperature if a very dense canopy approximates air temperature, a reasonable estimate of air temperature from remotely sensed measurements should be possible (Prihodko, and Howard, 1997). However, the relationship between T_a and vegetation indices is not always applicable is influenced by seasonality, ecosystem type and soil moisture variability (Sandholt et al, 2002; Benali et al, 2012). Surface energy balance is a new method to estimate T_a from T_S which focuses on physics. Energy balance is the sum of incoming atmospheric net radiation and anthropogenic heat fluxes, this method requires large amount of variable which often not provide by remote sensing data (Oke, 1987; Sun et al 2005; Brutsaert, 2005; Benali et al, 2012).

The objective of this study is estimating T_a based on T_S remote sensing using regression and energy balance approach. We estimated T_a in Jakarta city, Indonesia using MODIS data. Observation was done on dry season 2012 and emphasizing on urban feature.

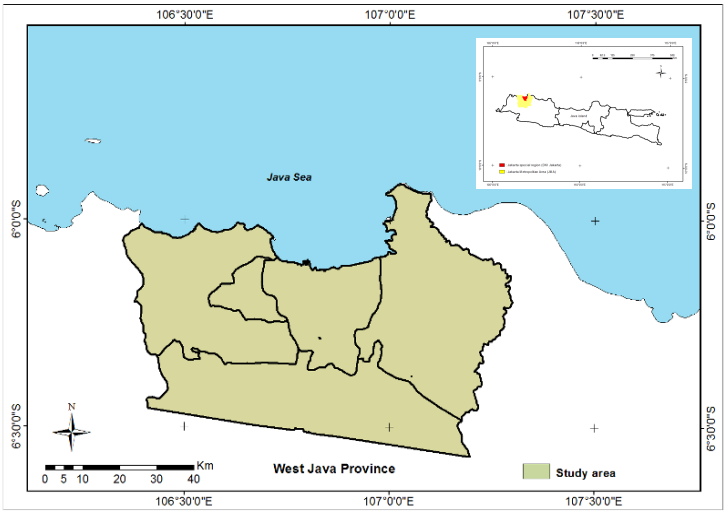

Figure 4. 1. Study area in Jakarta, Indonesia, urban area

4. 2. Material and Method

We used MODIS T_S data (Terra and Aqua) and applied different method to understand the sensitivity of each method. To validate present condition of T_S, as the

main component to estimate T_a , field observation was carried out during 18 – 26 September 2012.

4. 2. 1 . Land surface temperature (LST) in MODIS

Land surface temperature data at 1 km spatial resolution was downloaded from NASA's website, we use Aqua (daily) and Terra (8 days) T_S in dry season data (July – October) and validate it using field measurement in the same season and time closest to satellite overpass.

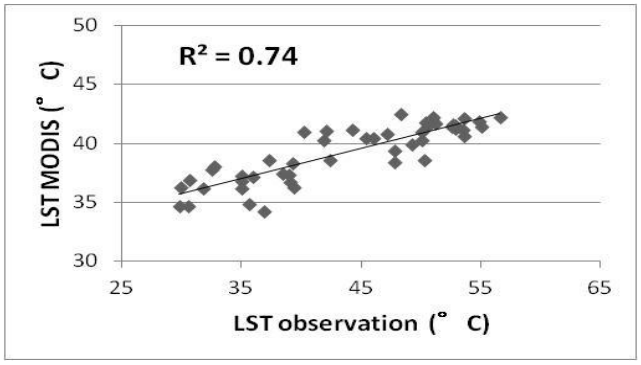

Figure 4. 2 Relationship between land-surface temperature (LST) derived from MODIS satellite data and from ground-based measurements.

Strong correlation was observed between the estimated LST using MODIS data and ground measurements. The determination coefficient (R^2) was 0.74; thus, the LST estimated by MODIS data provided a good representation of the actual LST in Jakarta (Mao, Qin, and Gong, 2005; Tursilowati et al., 2012). The LST was corrected based on regression relationships between the LST estimated by MODIS data and ground-based observations. The corrected LST distributions are shown in Fig 4.5.

4. 2. 2 . Air surface temperature (T_a) in MODIS

To compare the sensitivity of method in MODIS T_a estimation, we applied different method they are a simple regression and surface energy balance (SEB).

Based on regression LST – air temperature in MODIS

A simple regression method was applied to each corresponding sites between satellite and observation coordinate. The function is :

$$Y = ax + b \quad (1)$$

Where Y is air temperature and X is MODIS $T_{S.}$

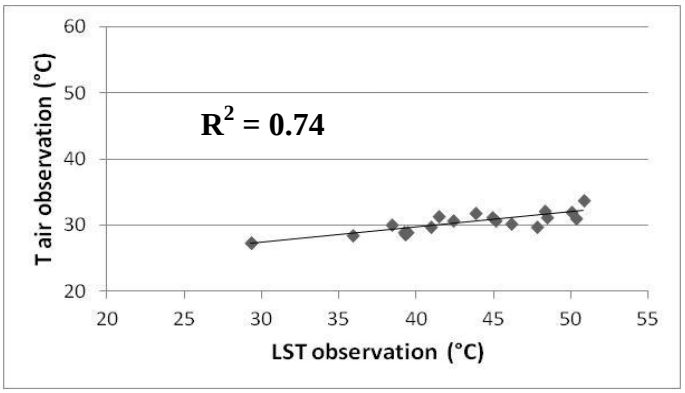

Figure 4. 3. Comparison between LST and air temperature observation (T_a) in ground based observation.

Surface energy balance in MODIS

Another method to estimate T_a in MODIS that we applied is SEB. Surface energy balance method is used to understand the energy and mass exchanged between the atmosphere and underlying surface with neglected vegetation feature in land surfaces. For natural land surface, absorbed net radiation should balance outgoing fluxes of ground heat, sensible heat, and latent heat. The function is:

$$Rn = LE + H + G \quad (2)$$

where Rn is net radiation, G is ground heat flux, LE is latent heat flux, and H is sensible heat flux.

$$Rn = (1- \alpha)\, Rs + \boldsymbol{\varepsilon}\boldsymbol{\varepsilon}_a + R_L\downarrow - \boldsymbol{\varepsilon}\, R_L\uparrow \quad (3)$$

where Rs is shortwave radiation (Wm^{-2}), $R_L\downarrow$ and $R_L\uparrow$ are the downward and upward blackbody radiation (Wm^{-2}), $\boldsymbol{\alpha}$ is surface albedo, $\boldsymbol{\varepsilon}_a$ is atmospheric emissivity, and $\boldsymbol{\varepsilon}$ is

the surface emissivity (Brutsaert, 2005; Kato, S and Yamaguchi, Y., 2005). In this study, climatology parameters was calculated from the ground station measurement on the AWS (Automatic Weather System), climatology station Pondok Betung (6 November 2012, 8:00.50 GMT, lat : -6.26°S; long : 106.75°E, http://aws-online.bmg.go.id/bmg/aws/index.php?id=1&long=107.4566650391&lat=-6.7994440079&z=8,).

$$\varepsilon_a = 1.24\left(\frac{e_a}{T_a}\right)^{1/7} \tag{4}$$

where T_a is athmospheric temperature (K), e_a is atmospheric water vapor pressure (hPa) (Brutsaert, 1982; Kato, S and Yamaguchi, Y., 2005).

$$G = Cg \times Rn \tag{5}$$

Table 4.1 Coefficient Cg used to calculate ground heat flux G for different surface coverage types and seasons

Land cover	Season		
	Spring	Summer	Winter
Bare soil	0.3	0.3	0.3
Field	0.3	0.3	0.3
Grassland or Rice field	0.1-0.3	0.1-0.3	0.1-0.3
Lawn	0.3	0.3	0.3
Forest	0.1	0.15	0.13
Suburban	0.7	0.4	1.0
Urban	0.7	0.4	1.0
Industrial	0.6	0.4	0.8

Each value was inferred from the measurement results for the heat fluxes (Brutsaert, 1982; Kato and Yamaguchi, 2005)

where Cg is coefficient, it`s fixed according to surface type and season, Rn is net radiation (Brutsaert, 2005; Kato, S and Yamaguchi, Y., 2005).

$$H = \boldsymbol{\rho} C_p (T_S - T_a) / r_a \tag{6}$$

where $\boldsymbol{\rho}$ is air density (kg/m^3), C_p is specific heat of air at constant pressure in J/kg K, Ts is surface temperature in K, H is sensible heat flux, Ta is air temperature (Brutsaert, 1982; Kato, S and Yamaguchi, Y., 2005).

$$r_a = \frac{\left(\frac{Z_m - d}{Z_{0m}}\right)\left(\frac{Z_h - d}{Z_{0h}}\right)}{k^2 U_z} \tag{7}$$

Where r_a is aerodynamic resistance (s/m), Zm is height of wind measurement (m), Zh is height of humidity measurement (m), d is zero plane displacement height (m), Z_{0m} is roughness length governing momentum transfer (m), Z_{0h} is roughness length governing transfer of heat and vapor (m), k is Von Karman`s constant (=0.4), is U_z is wind speed (Brutsaert, 2005; Kato, S and Yamaguchi, Y., 2005).

Table 4.2 Roughness length for different surface coverage types

Land cover	Z_{0M}	Z_{0M}/Z_{0H}
Water	$0.3*10^{-4}$	0.34
Bare soil	0.001	50
Field	0.004	50
Grassland or Rice field	0.1	100
Lawn	0.01	50
Forest	0.5-1.0	1000
Suburban	0.5	1000
Urban	1.5	1000
Industrial	0.9	1000

Kato and Yamaguchi, 2005

$$LE = \frac{\rho C_p}{\gamma r_a}(e_0 - e_a) \tag{8}$$

where e_0 is water vapor pressure (hPa), e_a is atmospheric water vapor pressure (hPa), ρ is air density (kg/m^3), Cp is air specific heat at constant pressure (1004 J/kg/K), γ is psychometric constant (hPa/K), r_a is aerodynamic resistance (s/m) eq. 6 (Brutsaert,

2005; Kato, S and Yamaguchi, Y., 2005). In this research latent heat flux is neglected based on the assumption that artificial land surfaces such as urban, suburban, industrial feature are dry.

The meteorological data used in this method were obtained from online meteorological agency such as solar radiation, and wind speed. Wind speed and solar radiation were assumed as constant in all study area. Finally, to estimate air temperature (T_a) by replaced eq. 4 and 5, we get:

$$T_a = T_s - \left(\frac{r_a R_n \left(1 - C_g R_n\right)}{\rho C_p}\right) \tag{9}$$

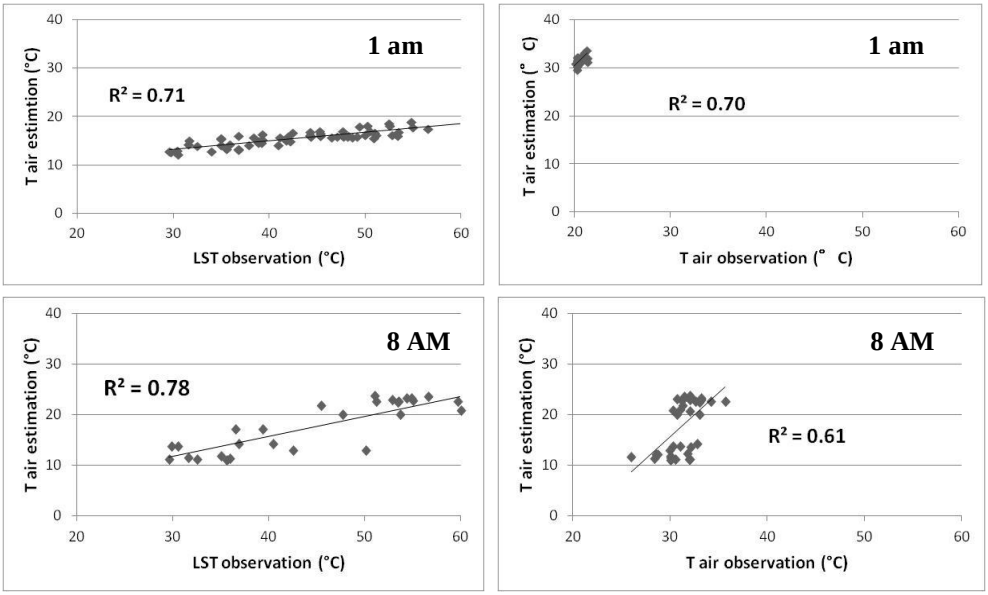

Figure 4. 4. Relationship between LST observation - air temperature estimation and air temperature estimation – air temperature observation using regression method in MODIS.

Some quite large differentiation between T_a estimation and T_a observation is occur in 8 AM data whereas the coefficient determination is high enough. T_a estimation seems to be lower than T_a observation, it could be happened that there is some biases

on this process that could not overcome by this method and data source. Thus, to minimize this weakness, a new method and data source is conducted.

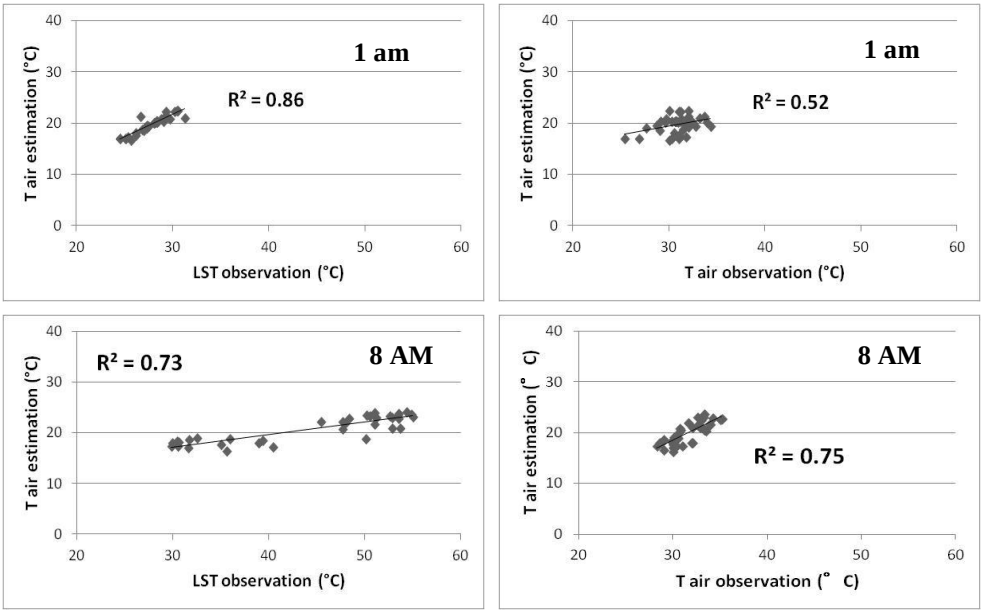

Figure 4. 5. Relationship between LST - air temperature estimation and air temperature estimation – air temperature observation using surface energy balance method in MODIS.

Figure 4. 4 and 4. 5 show a scatter plot of the relationship between T_a estimation and LST observation when applied to both methods. The determination coefficient (R^2) was high enough on each, and it also confirms that LST is representative enough to estimate T_a using these methods.

4. 3. Result and Discussion

To evaluate the sensitivity of regression and SEB method, we used daytime and night time MODIS data. Instantaneous T_a estimation was executed by applied the single regression equation in comparison between LST - T_a observation (Fig. 4.3) by using MODIS T_S. The validation showed that root mean square error (RMSE) on this method is 15.53 °C and T_a minimum – maximum value is 19.62°C – 22.49 °C for MODIS night time. The RMSE on daytime T_a estimation is lower than night time value, 11.69°C and minimum –maximum value is 21.55°C – 31.55°C. It reveals that by using regression method T_S MODIS data are weak to estimate T_a. Highest heat

concentration was distributing in central part of study area and spreading to the northwest area. The result showing above is acquired at the daytime within the same hour of satellite overpass at the local time.

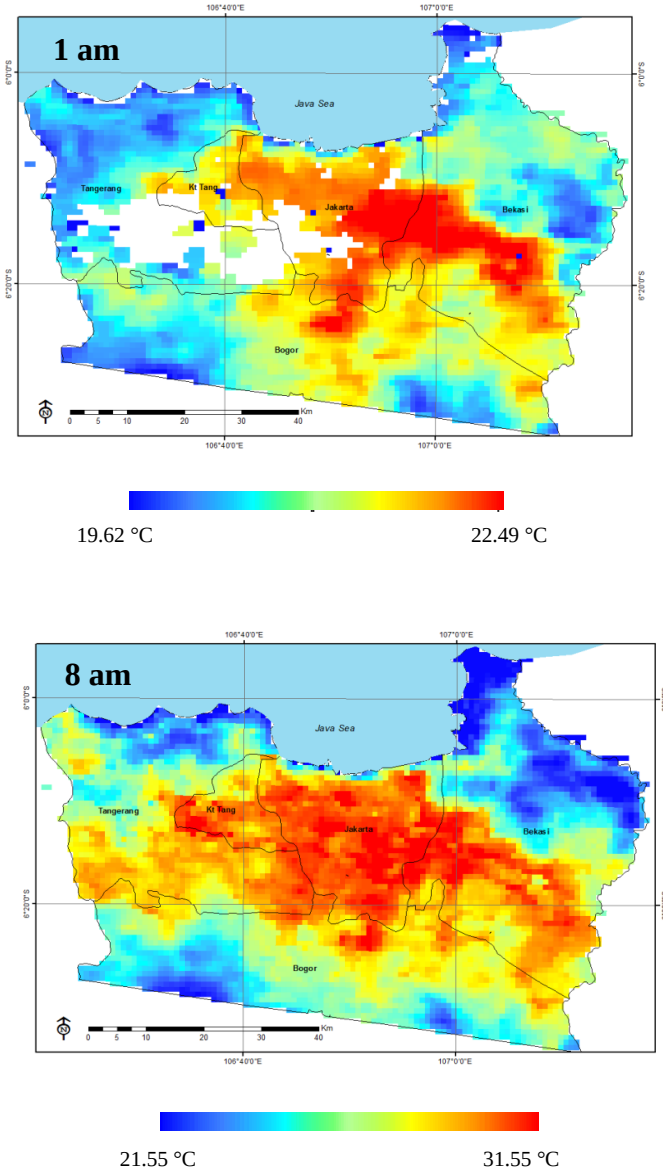

Figure 4. 6. Spatial distribution of air temperature (T_a) at Jakarta urban area using regression method.

Second method that we applied is surface energy balance method that adapted from the energy and mass exchanged between the atmosphere and earth surfaces (vegetation canopy or land surface without vegetation). Each SEB parameters that govern is explained in equation 2 – 9. Rn, wind speed parameter are collected from the

meteorology station and T_S was satellite data derivation. This research is emphasized on urban air estimation extraction from T_S remote sensing approach, as well as this reason the used of latent heat flux (eq. 8) is not calculated. We assumed that the urban, suburban or industrial surfaces are dry (Kato, and Yamaguchi, 2005). Figure 4.7 shows the T_a estimation in SEB MODIS image. We separate the urban surfaces by masking between urban and non-urban feature from land cover data.

Table 4.3 Root mean square error (RMSE), and coefficient correlation (R^2) in MODIS T_a estimation.

MODIS	1:00 AM		8:00 AM	
	R^2	RMSE (°C)	R^2	RMSE (°C)
REG	0.7	15.53	0.6	11.69
SEB	0.5	11.36	0.7	9.75

The result showed RMSE on SEB method is 9.75°C and T_a minimum - maximum is 25°C to 30°C for MODIS day time. The RMSE on T_a estimation is lower during night time, 11.36°C and minimum - maximum is 23.43°C – 25°C. Comparing with the RMSE value in SEB and regression method, SEB is seem to be smaller than regression method (table 4.2), it indicates that T_S MODIS in SEB method is perform well to estimate T_a. Here, some large biases occur in both data sets. One of possibility is the surface albedo (α) that use in Rn component in ground meteorological station is for the grass land, therefore, this method is applied in the urbanized area. Surface albedo is important in net radiation calculation, and grass land surfaces albedo is lower than dry soil or built-up surfaces. In the grass land surfaces, mostly, short wave radiation is absorbed while in the dry soil or built-up surfaces are reflected.

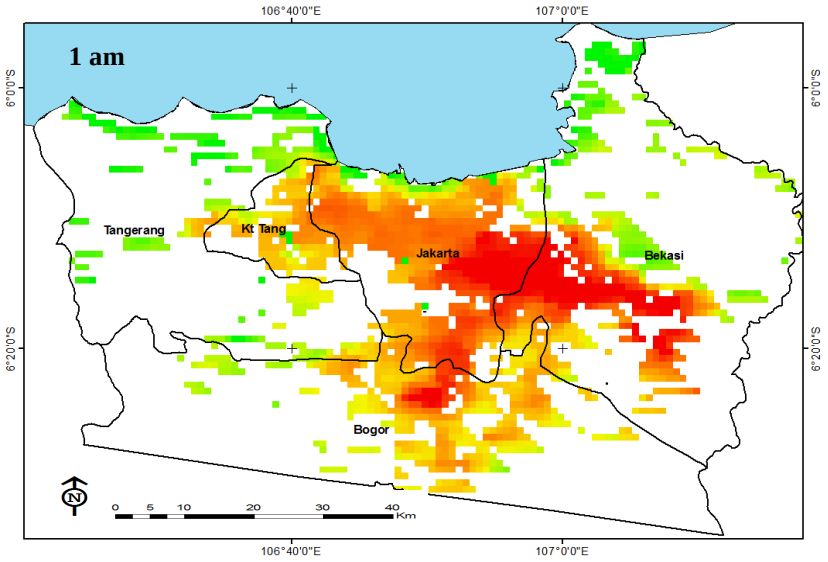

: Non urbanized area

23.43°C 25°C

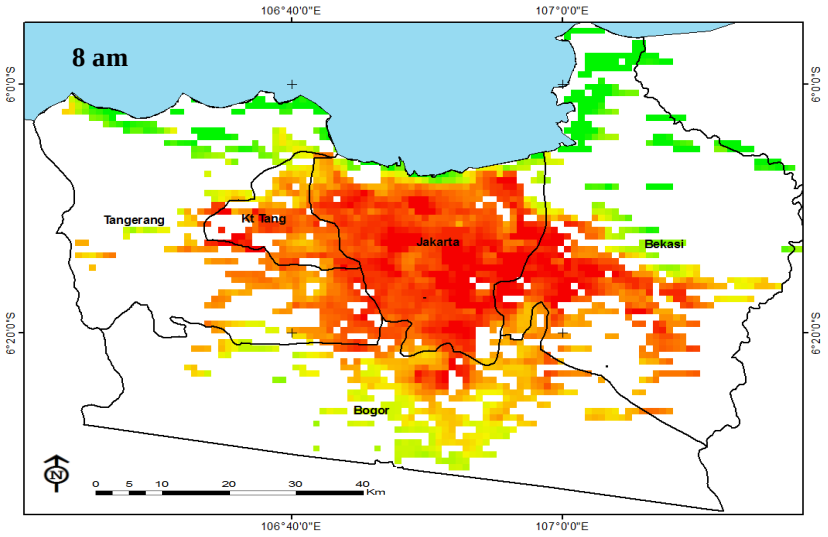

: Non urbanized area

25°C 30°C

Figure 4.7 Spatial distribution of air temperature (T_a) at Jakarta urban area using SEB method .

The tendency for range T_a estimation in regression method in both times is lower than range in SEB. This result also indicates that T_S MODIS day time or night time overpass were representative enough to estimate T_a in Jakarta city. Since large biases created in this study, more precise measurement is needed, particularly to calculate Rn components, surface albedo, short wave radiation, downward and upward blackbody radiation.

4. 4. Summary

The findings of this research can be conclude that surface energy balance on MODIS data is more reliable than simple regression method to estimate T_a from T_S remote sensing. The SEB RMSE shows 3 - 5 °C more sensitive than simple regression method when applied in Jakarta urban area. Both daytime and night time MODIS in 1 km spatial resolution were suitable to observe air temperature by combining between ground base measurement and surface temperature sensor. This study is emphasizing on the urban feature where wind speed and solar radiation were assumed as constant in all study area. In future, to test the effectiveness of the formula, modification on the Rn calculation is needed.

References

Benali, A., Carvalho, A.C., Nunes, J.P., Carvalhais, N., and Santos, A. Estimating air surface temperature in Portugal using MODIS LST data. *Remote Sensing of Environment*, 124 (2012), pp. 108–121.

Brutsaert, Wilfried. Hydrology An Introduction. New York : Cambridge University Press, 2005.

Colombi, Angelo., Michele, De, Carlo., Pepe, Monica., and Rampini, Anna. Estimation of daily mean air temperature from MODIS LST in Alpine areas. *Proceedings : European Association of Remote Sensing Laboratories (EARSel)*, 2007 pp. 38 – 46.

Fu, G., Shen, Z. X., Zhang, X. Z., Shi, P. L., Zhang, Y. J., & Wu, J. S. Estimating air temperature of an alpine meadow on the Northern Tibetan Plateau using MODIS and surface temperature. Acta Ecologica Sinica, 21, 8–13 (2011).

Jin, M., and Dickinson, E.R. Land surface skin temperature climatology: benefitting from the strengths of satellite observations. *Environmental Research Letters*, 5 (2010) 044004 (13 pp).

Kataoka, K., Matsumoto, F., Ichinose, T., and Taniguchi, M. Urban warming trends in several large Asian cities over the last 100 years. *Science of the Total Environment*, 407 (2009), pp. 3112– 3119.

Kato, S., and Yamaguchi, Y. Analysis of urban heat-island effects using ASTER and ETM+ data: separation of anthropogenic heat discharge and natural heat radiation from sensible heat flux. *Remote Sensing of Environment*, 99 (2005), pp. 44–45.

Kawashima, Shigeto., Ishida, Tomoyuki., Minomura, Mitsuo., and Miwa, Tetsuhisa. Relations between surface temperature and air temperature on a local scale during winter nights. *Journal of Applied Meteorology* Vol 39 pp.1570-1579.

Tursilowati, Laras., Tetuko, Josaphat., Kuze, Hiroaki., and Adiningsih, S. E. Relationship between Urban Heat Island Phenomenon and Land Use/Land Cover Changes in Jakarta – Indonesia. *Journal of Emerging Trends in Engineering and Applied Sciences*, 3 (4) 2012: 645 – 653.

Mao, K., Qin, Z., and Gong, P. A practical split-window algorithm for retrieving land-surface temperature from MODIS data. *International Journal of Remote Sensing*, Vol. 26 (2005) No. 15, pp. 3181–3204.

Oke, T.R. Boundary Layer Climates (2nd edition). Methuen : London and New York, 1987.

Prihodko, Lara., and Goward, N. Samuel. Estimation of air temperature from remotely sensed surface observations. *Remote Sensing and Environment* 60: 335 – 346 (1997).

Sandholt, Inge., Rasmussen, Kjeld., and Andersen, Jens. A simple interpretation of the surface temperature/vegetation index space for assessment of surface moisture status. *Remote Sensing of Environment* 79 (2002) 213– 224

Sun, J. Y., Wang, F. J., Zhang, H. R., Gilles, R.R., Xue, Y., and Bo, C. Y. Air temperature retrieval from remote sensing data based on thermodynamics. *Theoretical and Applied Climatology*, 80, 37 – 48 (2005).

Sobrino, A.J., Jimenez-Munoz, C.J., and Leonardo, P. Surface temperature and water vapour retrieval from MODIS data. *International Journal of Remote Sensing*, Vol. 24 (2003), No. 24, 5161-5182.

Stisen, Simon., Sandholt, Inge., Norgaard, Anette., Fensholt, Rasmus., Eklundh, Lars. Estimation of diurnal air temperature using MSG SEVIRI data in West Africa. *Remote Sensing of Environment* 110 (2007) 262 – 274.

Voogt, J.A, and Oke, T.R. Thermal remote sensing of urban climates. *Remote Sensing of Environment,* 86 (2003) 370–384.

Wenbin, Zhu., Aifeng, Lu., and Shaofeng, Jia. Estimation of daily maximum and minimum air temperature using MODIS land surface temperature products. *Remote Sensing of Environment* 130 (2013) 62 – 73.

CHAPTER 5

COMPARISON BETWEEN URBAN THERMAL ENVIRONMENT AND SOCIOECONOMIC CONDITION

5. 1. Introduction

Urban agglomeration and settlement are the most intensive forms of land use/land cover expansion. In recent years, horizontal urban extension is also influencing in a local climate changing, with consequent impacts on the health and quality of life of the residents. The conversion of the nature lands into impervious built-up lands is a result of rapid population growth. The study of the urban environment using remote sensing approaches to analyze the "urban quality of life" (QOL) has long been discussed (Lo and Faber, 1997, Li and Weng, 2007). In their research, physical and socioeconomic information was used as an input. Remote sensing also has been widely used as one of spatial data references such as urban land cover or land use mapping (Dewan, M. Ashraf, and Yamaguchi, Yasushi, 2009). Some researchers are also using vegetation and impervious surfaces indices in remote sensing to detect urbanization extension (Widyasamratri et al, 2013; Cui, and Shi, 2012; Yuan, and Bauer, 2007).

As indicated in many highly urbanized areas, urban heat island (UHI) is a major phenomenon which is observed in large cities as compared to its surroundings. Higher urban heat is mainly caused due to the anthropogenic heat released from vehicles, power plants, air conditioners and other heat sources, and due to the heat stored and re-radiated by massive and complex urban structures. Rapid growth of urban population and the changing of socio- economic pattern can be effected on thermal environment in some area. QOL is a concept that has no agreed on definition because a great variety of indicators can be used to measure it (Lo and Faber, 1997). Several studies agreed that QOL indicators were using socio-economic variables such as income, housing, education, and population (Rahman et al, 2011; Lo and Faber, 1997) and for environment indicator they using some ecological approaches such as vegetation indices, impervious surfaces indices, and ecosystem service valuation (Widyasamratri et al, 2013; Wu et al., 2012; Mennis, 2006; Lo and Faber, 1997).

5. 2. Data and Method

In 2006, the population density in Jakarta, the capital city in Indonesia, is 13, 526 inhabitants/km^2 (Susilo et al, 2007) while the population size in Jakarta metropolitan area was recorded at 8.4 million (Asri and Hidayat, 2005). The number of population is getting increase year by year and causing environmental degradation. The objective of present research is to investigate the relationship between socioeconomic status and urban thermal environment in Jakarta city, Indonesia.

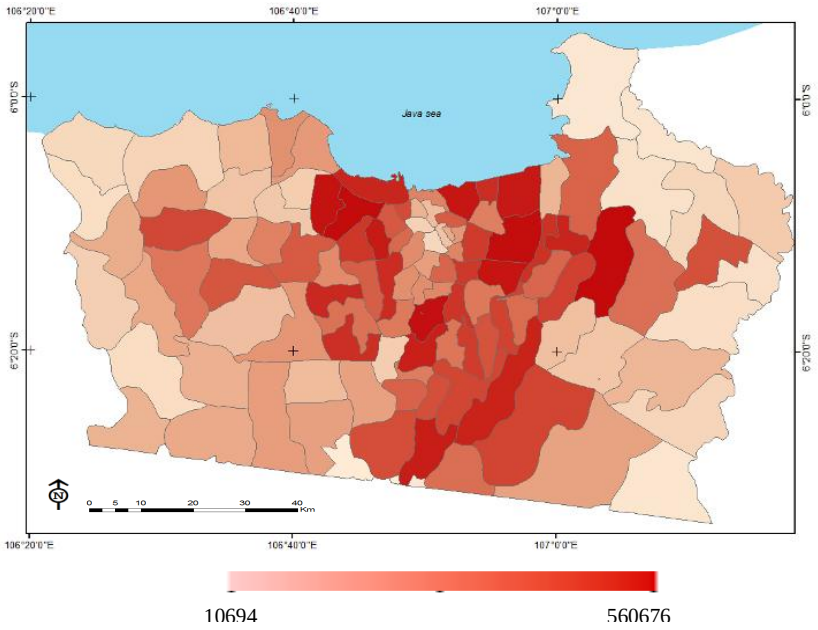

Figure 5. 1 Population distribution 2010 in Greater Jakarta

5. 2. 1. Data

The data sets used in this research are socioeconomic data sources derived from Indonesia village potential (PODES or Potensi Desa) in 2010 and air temperature (T_a) estimation from MODIS LST as the environment data. To analyze the relationship between environment and socioeconomic in Jakarta city, we used registered population, number of families which use electricity, poor families which get public health insurance (Jaminan Kesehatan Masyarakat or JAMKESMAS) , and letter of poor families identification (Kartu miskin) as the socioeconomic indicators.

5. 2. 2. Method

As the first step, T_a as the environmental component is summarized by applied surface energy balance method at 1 am, 8 am, 3 pm, and 6 pm MODIS LST data in

2012. Second, the variable then entered into a series of socioeconomic data to explore the relationship between environment component (T_a) and each explanatory socioeconomic variable. To assess the relationship between T_a and socioeconomic, weighted analysis in ArcGIS was applied. Overlay technique was executed to evaluate urban environmental livelihood in Jakarta. Qualitative weights were assigned to 5 selected parameters then composites it. Each parameters range was categorized by counting minimum and maximum value than divided into selected class.

Table 5.1 Parameter of urban environmental livelihood

Parameters	Category (persons)	Score	Source (unit)
Socioeconomic			PODES 2010, Statistic Bureau (village)
Population	10,694 - 148,193	10	
	148,194 - 285,693	20	
	285,694 - 423, 193	30	
	423, 194 - 560, 693	40	
Family using electricity	2,775 - 36, 284	4	
	36,285 - 70,094	6	
	70,095 - 103,604	8	
	103, 605 - 137,114	10	
Health insurance certificate for poor family	0 - 20,407	10	
	20, 408 - 40,815	8	
	40,816 - 61,224	6	
	61,225 - 81,632	4	
Poor family certificate	81 - 3,812	10	
	3,813 - 11,357	8	
	11,358 - 15, 089	6	
	15, 090 - 32, 045	4	
Environment			
Air temperature	20 - 23	10	Extracted from MODIS LST 2012 (pixel)
	24 - 27	20	
	28 - 31	30	
	32 - 35	40	

To analyze the relation between environment and socioeconomic aspect, we use indices that governed to assess household and welfare in Indonesia (Cahyat et al, 2007) and make some modification to synchronize it with our study. Whole process was executed in ArcGIS.

$$\frac{\Sigma score - score\,minimum}{\text{score maximum} - \text{score minimum}} x\ 100$$

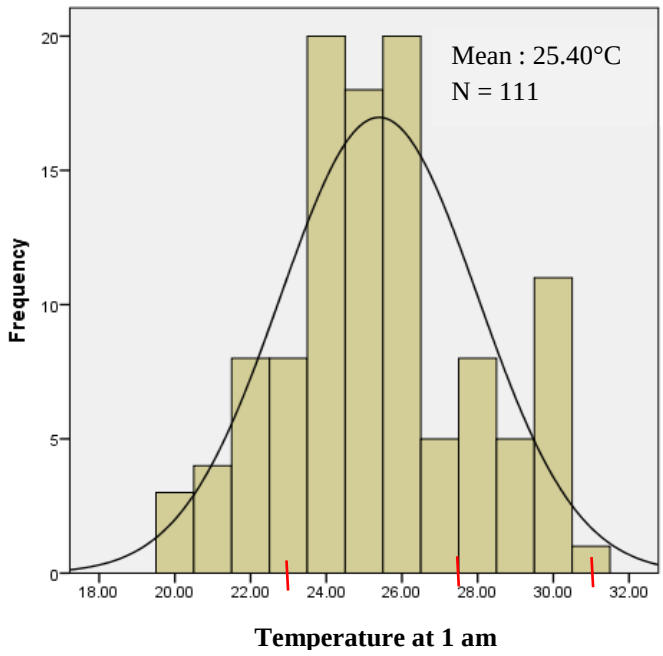

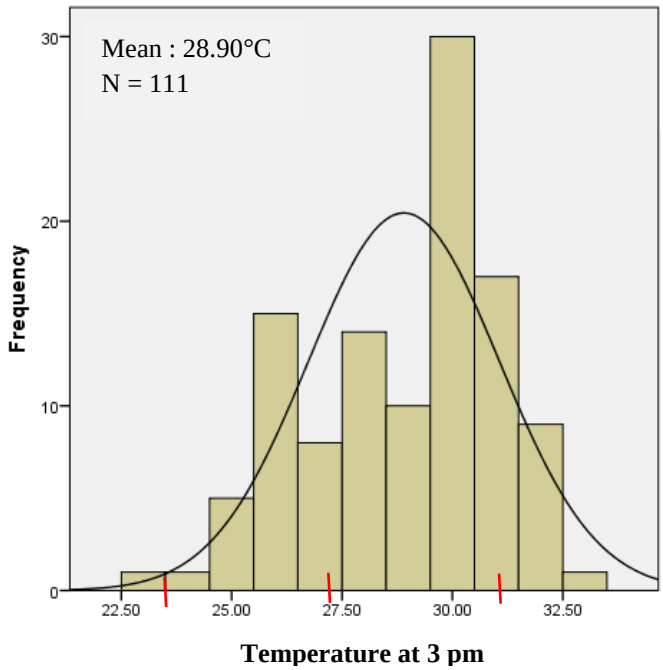

Figure 5.2 Histogram distribution of temperature at 1 am and 3 pm

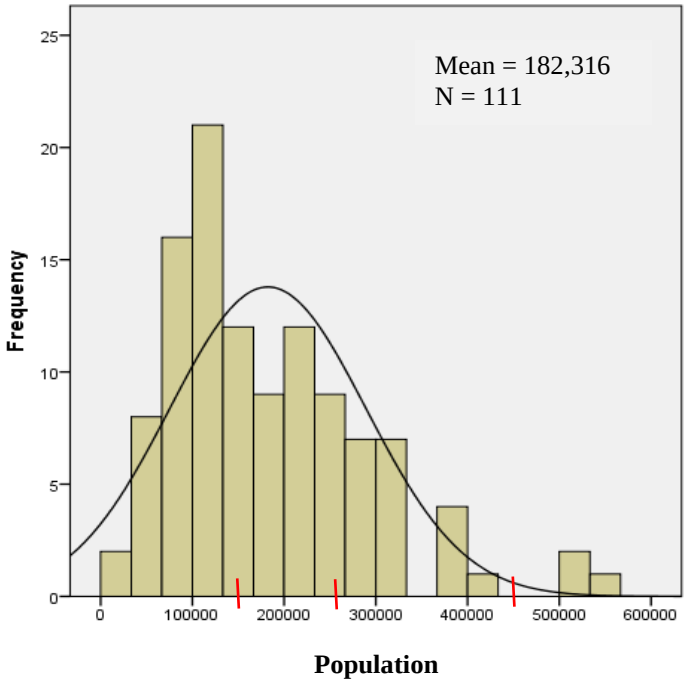

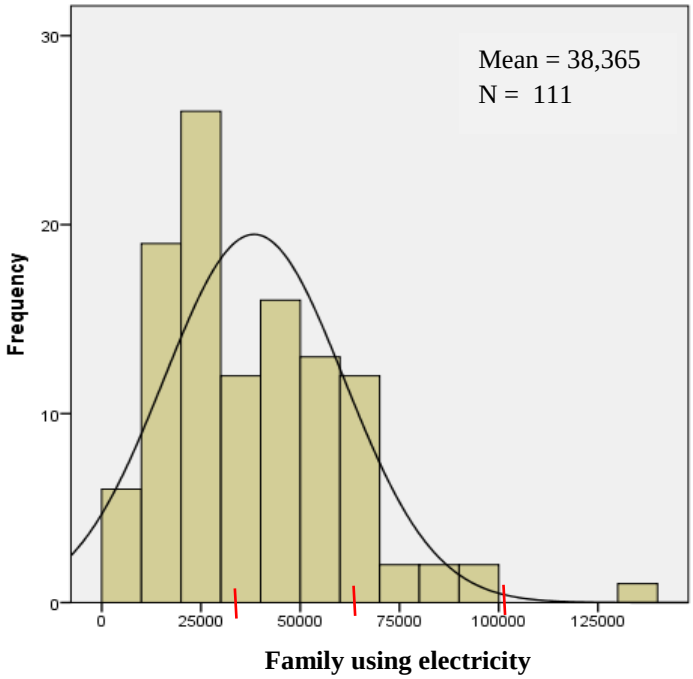

Figure 5.3 Histogram distribution of population and family using electricity

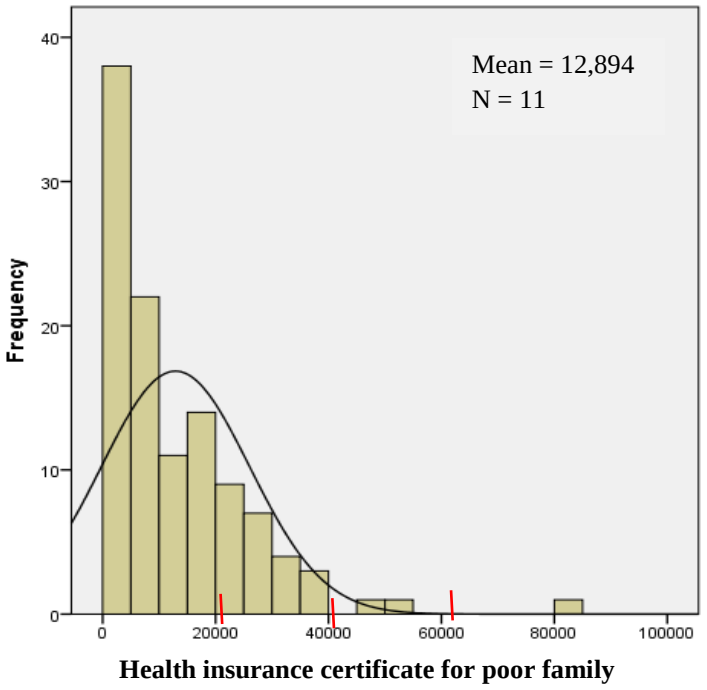

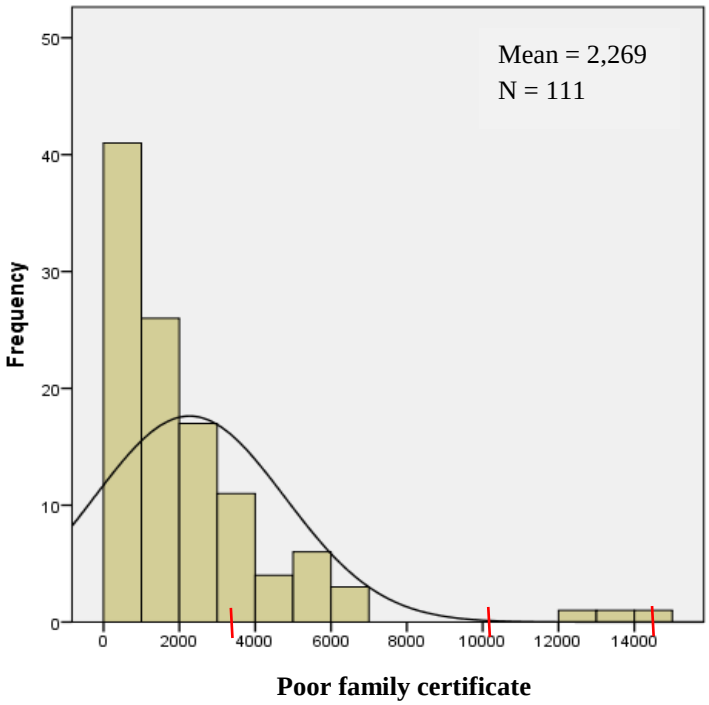

Figure 5.4 Histogram distribution of health insurance certificate for poor family and poor family certificate

Figure 5.2 – 5.4 are the histogram of air temperature data (1 am and 3 pm) and socioeconomic parameters. The histogram shows about frequency distribution in each threshold data where divided into the class (table 5.1). Figure 5.2 show that normally, in 1 am the air temperature is in 24.90°C – 25.88°C where the average is 25.40°C. In 3 pm air temperature data, the range is in 28.49°C – 29.30°C where the average is 28.90°C. Figure 5.3 is the histogram frequency of population and family using electricity. Population concentration range in Jakarta urban area is in 162,179 – 202,452 persons where the average population is 182, 316 persons. In Jakarta, there are 34,090 – 42,639 families using electricity in entire districts where the average is 38,365 populations. Figure 5.4 is the histogram frequency of health insurance certificate for poor family and poor family certificate in Jakarta urban area. There are 10,423 – 15,365 poor families who have health insurance certificate where the average numbers of families are 12,894 persons. For poor family certificate, there are 1,796 – 2,741 poor families who have certificate where the average number are 2, 269 persons.

5. 3. Result and Discussion

5.3.1 The relationship between Ta and population

Here, we used T_a as the environment parameter to evaluate the relationship between socioeconomic and environmental aspect to evaluate the urban physical condition. Result for the relationship between T_a and population are presented in Fig. 5. 5. The figure shows that there is a positive correlation between T_a and population, R^2 was slightly different depending on the time.

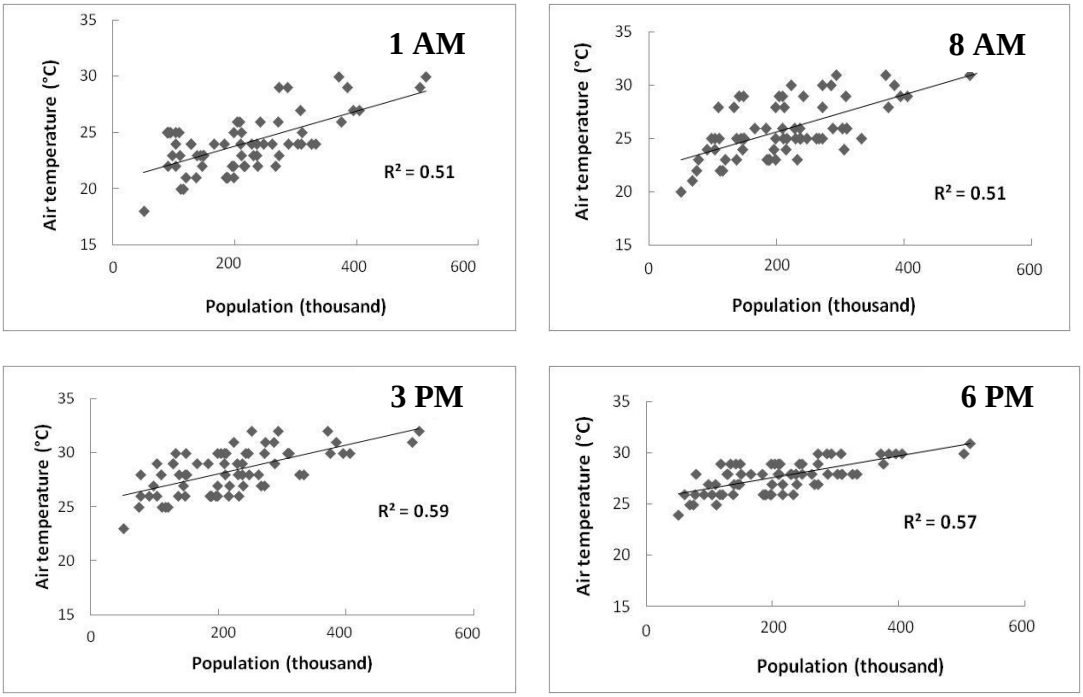

Figure 5. 5 Relationship between air temperature (T_a) and population in Jakarta within hours.

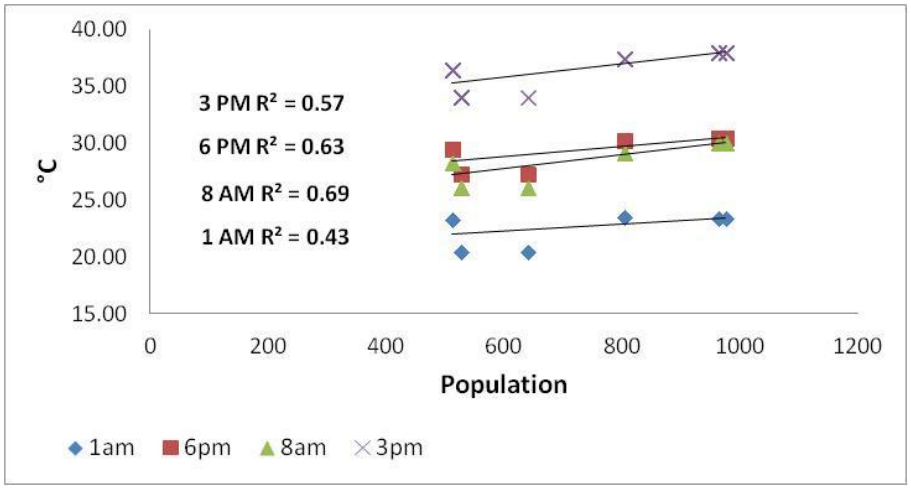

Figure 5. 6 Averaged air temperature (T_a) and population in Jakarta within hours.

The daily average of T_a and population shows strong relationship in each hour except in 1 am data (R^2 = 0.43). The weakness of coefficient determination in 1 am,

probably caused by the low air temperature and not much human activity during the night time.

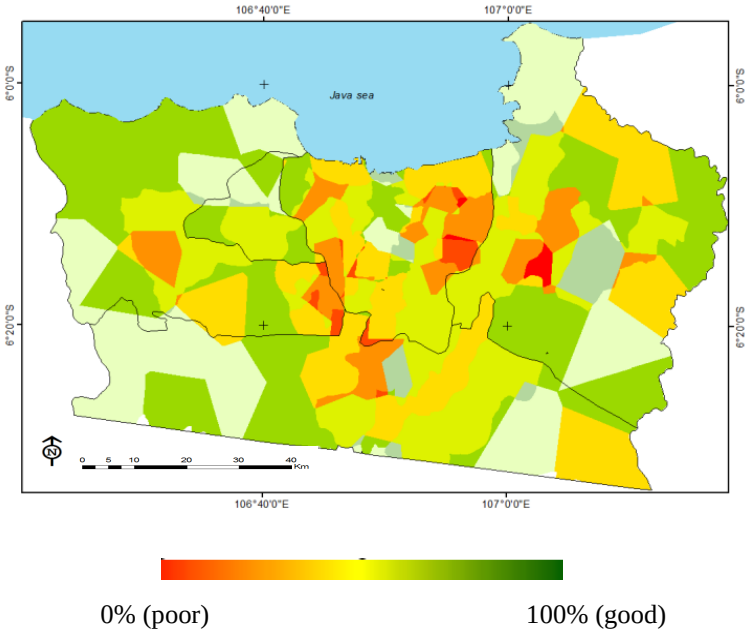

Figure 5. 7 Environment index in 1 am

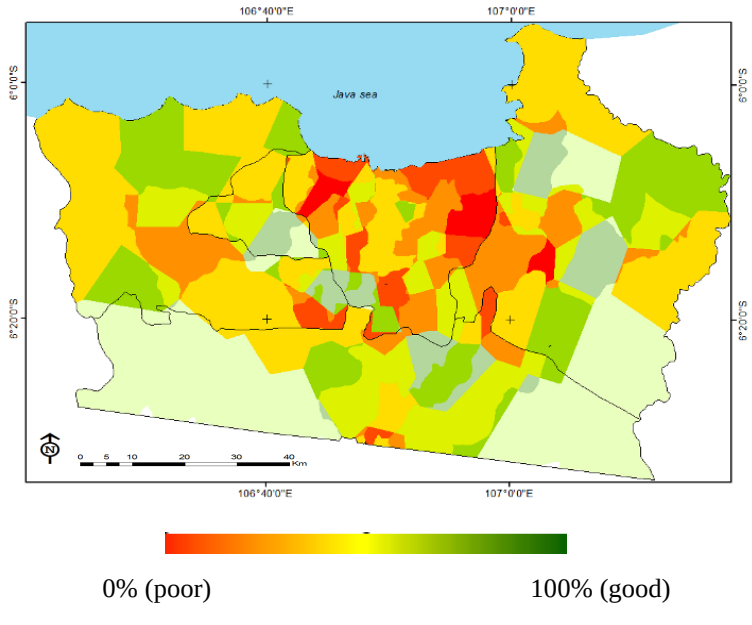

Figure 5. 8 Environment index in 3 pm

To understand the relation between environment and socioeconomic aspect, we used a GIS overlay technique to present those relationships. We defined as the good residential environment index by overlay T_a value and registered population data based on the strong relationship in each other. To represent the extreme, we just applied into two data hours, 1AM as the nighttime and 3 pm as the busy hour (Fig 5. 7 and 5. 8). The environment index range is between 0 % for low or bad value to 100% for high or good value. Population seems to be influencing enough to the environmental condition in urban area. It can be seen from the environment index (EI) in fig. 5.7 and 5.8. Figure 5. 7 shows that 83.6 % of whole area dominated by low EI (table 5.2). Nighttime, anthropogenic heat release is less and climatic effect is lower than in the daytime. However, urban center, as UHI indicated, 36.18% (table 5.3) of low EI is distribute in Jakarta city and it also affecting to the closest area (suburban)

Figure 5. 8 is the environment index in 3 pm which shows that 70% low EI is wider distributed in the whole area where 29.6 % is in Jakarta city (table 5.2 and 5.3). Daytime, as the busy hour has great environmental impact from the anthropogenic release. Generally, in the daytime low EI is well distributes to the whole area, suburban area also contribute to the poor EI.

Table 5.2 Environment index

Environment index			
1:00 AM	**Index**	**Quality**	**3:00 PM**
%			**%**
83.6	< 60	Poor	70
0	60 - 70	Minimum	0
11.7	71 - 80	Fair	20.5
4.4	> 80	Good	9.5

Table 5.3 Environment index for poor status

EI Poor status		
1:00 AM	**Area**	**3:00 PM**
%		**%**
36.1	Jakarta	29.6
20.6	Bogor	24.6
24.7	Tangerang	26.5
18.4	Bekasi	19.1

5.3.2 Urban socioeconomic

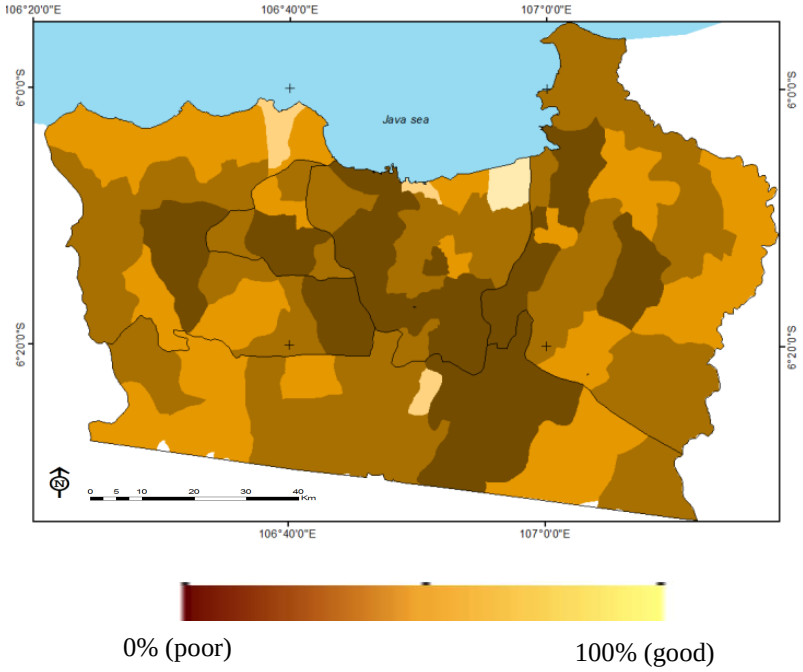

Figure 5. 9 Socioeconomic index

Socioeconomic index (SI) was created by overlaying socioeconomic parameters from PODES 2010 except population data. Socioeconomic condition is representing household and population welfare in study area. The results show that the 45.9 % areas are dominated by fair (moderate) condition S1 (table 5.4) where 37.7 % families are living in Jakarta city and followed by Bogor (23.5%) (table 5.5).

Table 5.4 Socioeconomic index

Socioeconomic index		
Index	**Quality**	**%**
< 60	Poor	1.6
60 - 70	Minimum	19.8
71 - 80	Fair	45.9
> 80	Good	30.6

Table 5.5 Socioeconomic index for fair status

SI fair status	
Area	**%**
Jakarta	37.3
Bogor	23.5
Tangerang	19.6
Bekasi	19.6

5.3.3 Urban environment livelihood (ULI)

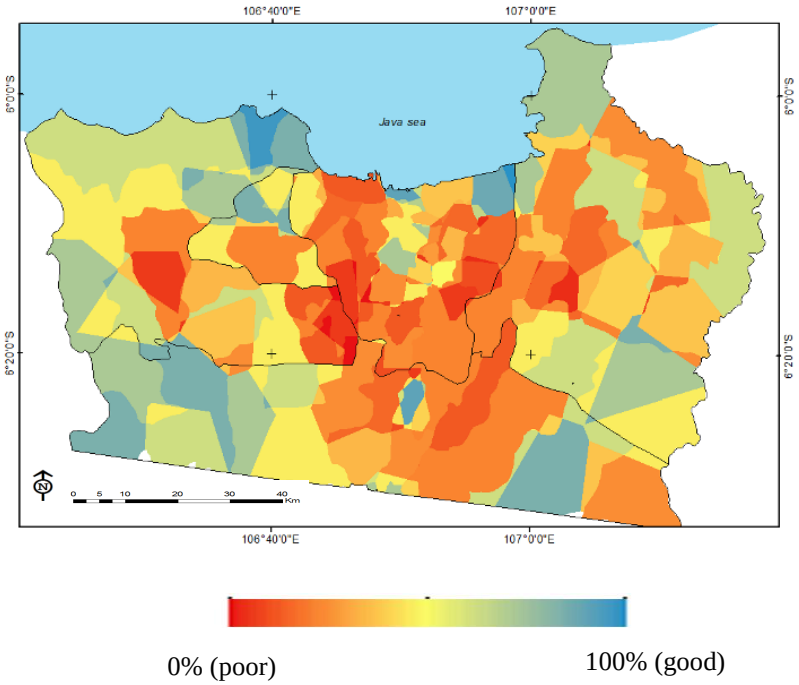

Figure 5. 10 Urban environment livelihood index in 1 am

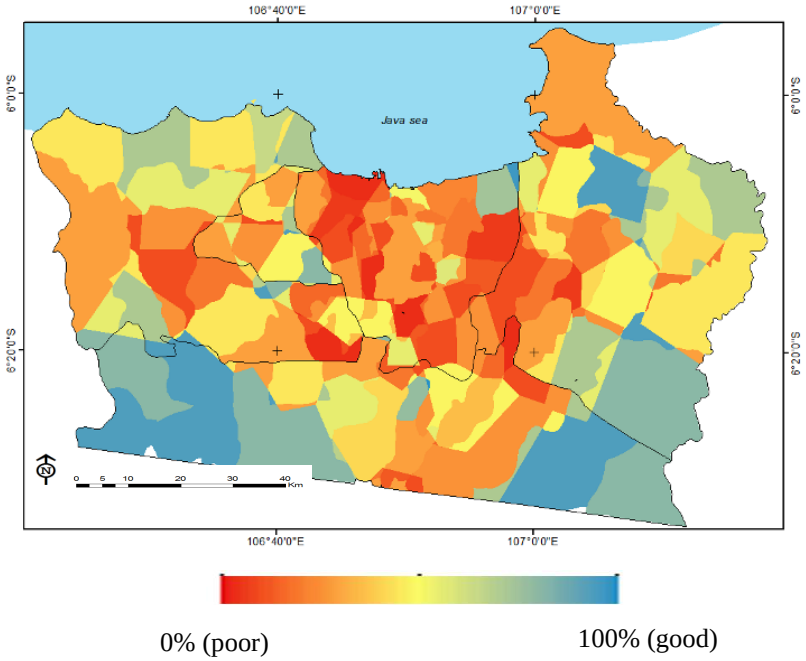

Figure 5. 11 Urban environment livelihood index in 3 pm

Finally, synthesis results from environment and socioeconomic indices are shown in fig. 5.10 and 5.11. Urban livelihood index (ULI) is the index which used to measure the urban socio-environment condition in urban area. By combine socioeconomic and environment status this index is defined.

Table 5.6 Urban livelihood index

Urban livelihood index			
1:00 AM	**Index**	**Quality**	**3:00 PM**
%			**%**
47.7	< 60	Poor	47
22.5	60 - 70	Minimum	15.8
22.8	71 - 80	Fair	20.4
7	> 80	Good	16.8

At nighttime, 47.7 % areas are dominated by poor quality ULI where 32% are in Jakarta city and followed by Tangerang. In the daytime whole areas are contributes to the low quality (47%), where the concentration of low quality ULI is strongly identified in Jakarta as inner urban (40.4%) which shown in table 5.9 and 5.10.

Table 5.7 Urban livelihood index for poor status

ULI poor status		
1:00 AM	**Area**	**3:00 PM**
%		**%**
32	Jakarta	40.4
22.2	Bogor	19.7
24.8	Tangerang	26.2
21	Bekasi	13.7

During the night time and peak time, both, urban area has low quality environment livelihood. It can be seen from the solid fine color in the urban center are dominated by solid fine color which representing low index. The 1 am result shows that low environment livelihood index is in urban center to the southern part (suburban) while in 3 pm as the peak hour; low environment livelihood is spread over to the whole area. It can be identified that there are some movement activity among the urban population and reflect to the pattern change of environment livelihood index. ULI indicates how strong urban area socio-environment quality is. The analysis shows that increasing thermal status followed by decreasing ULI it is characterized by lower EI and SI. It can be seen from the degree of ULI distribution at nighttime (fig 5.10) and daytime (fig 5.11).

In previous study, relationship between socioeconomic status and urban environment condition in Georgia, USA, found that low environment quality is characterized by high surface temperature, high population density, low percentage of vegetation coverage, and low income value is located in urban area (Lo and Faber, 1997). In Semarang, Indonesia, purely remote sensing approaches was used to evaluate urban environment by using vegetation and urban indices where low environment quality is characterized by low ratio vegetation cover and high income value (Widyasamratri, 2013). In Jakarta, we used direct measurement of air temperature and applied it into remote sensing data, then, by combine with statistic data we evaluated urban environment condition. Most previous study revealed that low environment quality is indicated by low vegetation coverage, high surface temperature, and high population.

5. 4. Summary

This research has demonstrates that there was a relationship between physical environmental and socioeconomic data in Jakarta urban area. Physical parameter can be extracted directly from MODIS LST data to estimate T_a by using remote sensing approach and socioeconomic parameters are extracted from statistic database. T_a as the environment parameter has strong relationship with population which indicated from high coefficient correlation in whole hours. The comparison of average T_a and population also indicate that those parameters have close relationship.

The two integration approaches in this research to measure the impact of urbanization using environment and socioeconomic indices were developed. The result shows that urban area is the most threatened by low quality of environment life. It indicated from the distribution of low socioeconomic and environment indices that concentrate to the inner urban area. This urban environment livelihood index can represent the relationship between urban physical (thermal environment) and socio economic condition in the Jakarta urban area.

References

Asri, Umamil, Dail., and Hidayat, Budi. Current transportation issues in Jakarta and its impacts on environment. *Proceedings of the Eastern Asia Society for Transportation Studies*, Vol. 5, pp. 1792 - 1798, 2005.

Cahyat, Ade., Gonner, Christian., and Haug, Michaela. 2007. Mengkaji Kemiskinan dan Kesejahteraan Rumah Tangga. Center for International Forestry Research, Indonesia. pp. 73 – 83.

Cui, Linli., and Shi, Jun. Urbanization and its environmental effects in Shanghai, China. *Urban Climate* 2 (2012) 1–15.

Dewan, M. Ashraf, and Yamaguchi, Yasushi. Land use and land cover change in Greater Dhaka, Bangladesh: Using remote sensing to promote sustainable urbanization. *Applied Geography* 29 (2009) 390–401

Li, G, and Weng, Q,. Measuring the Quality of Life in City of Indianapolis by Integration of Remote Sensing and Cencus Data. *International Journal of Remote Sensing. Vol. 28, No. 2, P. 249 – 267.*

Lo, C.P, and Faber, J. Benjamin(1997). Integration of Landsat Thematic Mapper and Cencus Data for Quality of Life Assesment. *Remote Sensing Environment Journal, 62: 143-157 (2007).*

Mennis, Jeremy. Socioeconomic-vegetation relationship in urban, residential land : the case of Denver, Colorado. *Photogrammetric Engineering & Remote Sensing*. Vol. 72, No. 8, August, 2006, pp. 911 – 921.

Rahman, Atiqur., Kumar, Yogesh., Fazal, Shahab., and Bhaskaran, Sunil. Urbanization and Quality of Urban Environment Using Remote Sensing and GIS Techniques in East Delhi- India. *Journal of Geographic Information System*, 2011, 3, 62-84.

Steinberg, Florian. Jakarta: Environmental problems and sustainability. *Habitat International* 31 (2007) 354–365.

Susilo, O, Yusak., Santosa, Wimpy., Joewono, Basuki, Tri., and Parikesit, Bambang. A reflection of motorization and public transport in jakarta metropolitan area. *IATSS research.* Vol.31 No.1, 2007 pp 59 – 68.

Widyasamratri, Hasti., Suharyadi, R., Souma, Kazuyoshi., and Suetsugi, Tadashi. Analysis of Urban Environmental Conditions Based on Satellite Remote Sensing and Socioeconomic Conditions Based on Statistics—A Case Study of Semarang Municipality, Indonesia. *Journal of Environmental Science and Engineering* B 2 (2013) 398-405.

Wu, Kai-ya., Ye, Xin-Yue., Qi, Zhi-fang., and Zhang, Hao. Impacts of land use/land cover change and socioeconomic development on regional ecosystem services: The case of fast-growing Hangzhou metropolitan area, China. *Cities* 31 (2013) 276–284.

Yuan, Fei, and Bauer, E. marvin. Comparison of impervious surface area and normalized difference vegetation index as indicators of surface urban heat island effects in Landsat imagery. *Remote Sensing of Environment* 106 (2007) 375–386.

CHAPTER 6

CONCLUSIONS

This study is revealing how urbanization is effecting in local climate and urban environmental life. Three main aspects are conducting to analyze the urban environment through air temperature estimation. They are, recognizing land cover distribution, air temperature estimation from remote sensing approach, and detecting socioeconomic related to physical environment pattern within study area. The important findings from this research are summarized as the following:

Chapter 2 :

Urban development which reduces green area to built area will effect on local climate condition. Urbanization in Jakarta becomes wider and spreading to the neighboring city such as Depok, Bogor, Tangerang, and Bekasi, and well known as Jakarta Metropolitan Area (JMA). To understand the land cover distribution and remote sensing validation for meteorological situation during dry season, field observation was conducted in Jakarta in September – October 2012.

The result shows that strong thermal environment was detected in urban centers. High difference range of air temperature was happened between urban and suburban area which indicate urban heat island (UHI) effect. The difference of urbanized area was recognized from the land cover in 1989 and 2006 from satellite image. The land cover distribution shows that intensive urbanization occurs.

Chapter 3 :

In order to estimate T_a from Landsat T_S approach, we applied a simple regression method to Landsat 1989 and 2006. Higher T_a average was detected in 1989 than 2006 data with the difference is 5-7 °C. In this study, we are emphasizing on the affectivity of Landsat T_S to estimate T_a and neglected the land use or topographic aspects. Our study revealed that high determination coefficient (R^2) between T_a and LST in ground-based measurements indicate that remote sensing thermal data can be used as an indicator of T_a and also can overcome spatial problem of T_a estimation.

Chapter 4:

In order to get the smallest error of air temperature estimation from remote sensing approach, we were comparing with two different methods which applied in MODIS thermal data. First method is a simple regression, and second method is a surface energy balance. The result shows that surface energy balance (SEB) on MODIS data is more sensitive than simple regression method to estimate T_a from T_S remote sensing. It indicated from the smaller RMSE on SEB than simple regression method. RMSE by SEB is 3 - 5°C more sensitive than in simple regression method in daytime and nighttime satellite data records. However, both times satellite data can be used to estimate T_a by combining with ground base meteorological record. Solar radiation and wind speed is assumed in constant value, future, to test the effectiveness of the formula, modification on the solar radiation calculation is needed.

Chapter 5:

To analyze the relationship between physical environment and socioeconomic condition in Jakarta, we compare with thermal data from MODIS satellite and statistical data from statistic bureau database. The result shows that population has strong relationship with thermal environment. It indicated from high coefficient determination (R^2) in comparison scatter diagram between populations - T_a. To integrate thermal environment and socioeconomic data, we governed some indices that explain the spatial distribution of urban environment life. Urban area is the most threatened condition of low environment caused by high population concentration and high thermal degree. However, this research needs more improvement to conduct better result in urban environment from the usage of electricity or fuel.

Hence, based on the result, I conclude that MODIS T_S data is more effective to estimate T_a in order to overcome spatial lack of ground base meteorological station than Landsat. The small error in estimation can be minimized by applied SEB method on daytime or nighttime MODIS data. In order to detect the impact of urbanization, the usage of thermal data from remote sensing as the environmental parameter is suitable enough. Then, to understand the urban environment livelihood, statistical data as the socioeconomic parameter is needed. However, the uses of statistical data is not enough

to understand the physical urban environment, then, we introduce environment index determined from thermal status. The results indicate that urban area is the most threatened of low environmental life caused by the high concentration of urban heat and urban poor family which living in an inner core area. Urban area has the good socioeconomic condition, but thermal environment is worse. The categorization of the indices is needed to evaluating the degree of environment value on urban area.